Renewable and Sustainable Energy Reviews 36 (2014) 34–51

Contents lists available at ScienceDirect

Renewable and Sustainable Energy Reviews

journal homepage: www.elsevier.com/locate/rser

Clathrate hydrate technology for cold storage in air conditioning systems

Xiaolin Wang*, Mike Dennis, Liangzhuo Hou

College of Engineering and Computer Science, Australian National University, Canberra 2601, Australia

ARTICLE INFO

Article history:
Received 27 August 2013
Accepted 7 April 2014
Available online 4 May 2014

Keywords:
Clathrate hydrate
Cold storage air conditioning system
Improvement method
System performance

ABSTRACT

Clathrate hydrate is an attractive technology for cold storage applications. It offers a high cold storage density and elevates the phase change temperature compared to water. It offers better heat transfer properties and improved cyclic stability compared to eutectic salts. This paper reviews previous work on clathrate hydrates as phase change materials (PCMs) for cold storage air conditioning applications. Three aspects have been focused on: the characteristics of clathrate hydrates, modification of clathrate hydrate properties, and practical utilization of clathrate hydrates as cold storage media. Specifically, refrigerant clathrate hydrates, CO_2 hydrates, hydrocarbon clathrate hydrates and multi-component clathrate hydrates are introduced. Technologies to decrease equilibrium pressure, increase dissociation enthalpy, accelerate formation process, decrease supercooling extent and enhance gas solubility are summarized. Clathrate hydrates based cold storage air conditioning systems that transport cooling in a manner of fixed container as well as in hydrate slurry are reviewed, and optimizing methods of system performance are studied. Finally, four features of clathrate hydrates, namely the self-preservation effect, memory effect, gas conversion and hydrate structure transformation are discussed.

Contents

1. Introduction . . . 35
2. Clathrate hydrates . . . 35
   2.1. Refrigerant clathrate hydrates . . . 35
   2.2. CO_2 clathrate hydrate . . . 36
   2.3. Hydrocarbon clathrate hydrates . . . 36
   2.4. Multi-component clathrate hydrates . . . 37
      2.4.1. Multi-component system of refrigerant clathrate hydrates . . . 37
      2.4.2. Multi-component system of hydrocarbon clathrate hydrates . . . 37
      2.4.3. Multi-component system of CO_2/N_2 and hydrocarbon clathrate hydrates . . . 38
3. Modification of clathrate hydrates . . . 38
   3.1. Decrease of equilibrium pressure . . . 38
   3.2. Increase of dissociation enthalpy . . . 40
   3.3. Acceleration of formation process . . . 41
      3.3.1. Mechanical agitation and magnetic interference . . . 42
      3.3.2. Additives . . . 42
      3.3.3. Structural optimization of the reactor . . . 42
   3.4. Decrease of supercooling extent . . . 44
   3.5. Enhancement of gas phase solubility . . . 44
4. Clathrate hydrates for cold storage air conditioning applications . . . 44
   4.1. Clathrate hydrate based cold storage air conditioning systems . . . 44
   4.2. Improvement methods of charging and discharging performance . . . 45
   4.3. Clathrate hydrate slurry . . . 46

* Corresponding author. Tel.: +61 2 61251975.
E-mail address: xiaolin.wang@anu.edu.au (X. Wang).

http://dx.doi.org/10.1016/j.rser.2014.04.032
1364-0321/

5. Promising features of clathrate hydrates as cold storage media . . . 46
5.1. Self-preservation effect . . . 46
5.2. Memory effect . . . 47
5.3. Gas conversion. . . . 47
5.4. Hydrate structure transformation . . . 47
6. Conclusions . . . 48
References . . . 48

1. Introduction

Air conditioners equipped with cold storage offers a means to alleviate peak loading on electricity grids and to utilize power in off peak periods. Water and ice are the most commonly used cold storage media, for their low price and safety. However, liquid water has an intrinsic low cold storage density, thus a large storage volume is needed to achieve the required cold storage capacity. Ice melts and freezes at 0 °C, therefore the chiller has to work at low evaporating temperatures, resulting in an inferior Coefficient of Performance (CoP). By contrast, clathrate hydrates commonly have a latent heat of phase change close to that of ice, and a phase change temperature of 5–12 °C that matches well with the operating conditions of conventional air conditioning systems. Moreover, clathrate hydrate could enable direct contact charging and discharging, thus dramatically improving the heat transfer efficiency to and from a cold store. Clathrate hydrate manifests obvious advantages over conventional cold storage media (Table 1), thus is considered to be a promising candidate for cold storage and has sprouted numerous investigations [1].

Clathrate hydrates are crystalline solid compounds formed from water and gas molecules. The gas molecules (guest) are trapped in cages that are composed of hydrogen-bounded water molecules (host) [2]. The guest gas is usually a refrigerant gas, natural gas or other small gas molecule. The former is specified in this work as the gas of conventional refrigerant, namely chloro-fluoro-carbons (CFCs), hydro-chloro-fluoro-carbons (HCFCs) or hydro-fluoro-carbons (HFCs); the latter refers to terrestrial gases and mineral gases, typically including CO_2, N_2 and hydrocarbon gases [3]. Molecular properties of some featured guest gases are listed in Table 2 [4].

The aim of this work is to present a review of research progress on clathrate hydrates as PCMs in cold storage air conditioning systems, concerning the formation/dissociation conditions, optimizations and applications of various clathrate hydrates. Refrigerant clathrate hydrates, CO_2 clathrate hydrates, hydrocarbon clathrate hydrates, and multi-component clathrate hydrates are introduced in detail. Technologies to decrease the equilibrium pressure, increase dissociation enthalpy, accelerate formation process, decrease super-cooling effect and enhance gas solubility are analyzed. Moreover, clathrate hydrate based cold storage air conditioning systems that transport cooling in a manner of fixed container as well as clathrate hydrate slurry are studied for practical system design and optimization.

Table 1
Performance and economical features of different cold storage media.

Cold storage medium	Water	Ice	Eutectic salt	Clathrate hydrates
Phase change temperature	0–10	0	8–12	5–12
CoP of refrigerator	1	0.6–0.7	0.92–0.95	0.89–1
Heat transfer performance	Superior	Medium	Inferior	Superior
Investment	< 0.6	1	1.3–2	1.2–1.5

2. Clathrate hydrates

Fundamental studies of clathrate hydrates generally concerns the following properties:

- the phase equilibrium conditions, for the compatibility with the operating conditions of cold storage systems;
- the phase change enthalpy, for evaluating the cold storage capacity;
- the hydrate nucleation and growth rate, for predicting the cold storage rate.

Van der Waals–Platteeuw solid solution theory is commonly used for theoretical studies of phase equilibrium behavior of clathrate hydrates [5]; while for experimental measurements, an apparatus including of a high-pressure cell was usually employed [6,7]. The dissociation enthalpy can be calculated by Clapeyron equation based on experimental data, or directly measured by an insulated boil-off chamber in a constant temperature bath [8].

2.1. Refrigerant clathrate hydrates

Most refrigerant gases can form clathrate hydrates under supportive conditions. However, CFCs and HCFCs have been gradually prohibited due to their ozone depletion potential and greenhouse impact. In contrast, HFCs clathrate hydrates have been widely studied since 1992 when CFCs phase out began to be implemented [9]. Equilibrium data of HFC-134a, HFC-125 and HFC-143a hydrate were measured by Hashimoto et al. [7], showing that HFC-134a hydrate had the lowest equilibrium pressure. The dissociation enthalpies of the three HFCs hydrates were all about

Table 2
Molecular properties of guest gases.

Guest	Structure	Hydrate dissociation pressure at 273 K (MPa)	Melting temperature (K)	Boiling temperature (K)	V (A^3)	Max length (A)
CH_3F	sI	0.2	131	195	33.5	4.7
CH_2F_2	sI	0.2	137	221	38.9	5.2
CHF_3	sI	0.3	118	191	42.9	5.2
CF_4	sI	4.2	89	145	49.4	5.3
CH_4	sI	2.5	91	112	28.6	4.3
C_2H_6	sI	0.5	90	185	45.6	5.6
C_3H_8	sII	0.2	85	231	62.4	6.7
CO_2	sI	1.2	195	\	33.3	5.4
H_2S	sI	0.1	188	213	25.2	3.8
O_2	sII	11.9	55	90	20.6	3.9
N_2	sII	15.9	63	77	21.7	3.9
Ar	sII	10.5	84	87	27.8	1.9
Kr	sII	1.5	116	120	34.5	2.0
Xe	sI	0.2	161	165	42.2	2.2

Table 3
Properties of refrigerant gases.

Guest gas	Molecular formula	Critical temperature (°C)	Critical pressure (MPa)	Enthalpy of reaction (kJ kg^{-1})	Solubility (g kg^{-1}) (water) (25 °C)	ODP	GWP (100 yr)	Re
HCFC-141b	CH_3CCl_2F	204.15	4.25	344	0.509	0.086	700	[11]
HCFC-142b	CH_3CClF_2	136.45	22.80	349	0.14	0.043	2400	
HFC-134a	CH_2FCF_3	101.06	4.059	358	0.15	0	1300	[9,11–16]
HFC-143a	CH_3CF_3	72.89	3.776	383.9	\	0	3800	[13,14]
HFC-125	CHF_2CF_3	66.25	3.631	362	0.09	0	3400	[9,12,14,15,18]
HFC-152a	CH_3CHF_2	113.26	4.517	383	0.28	0	120	[11–14,18,19]
HFC-227ea	CF_3CHFCF_3	102.8	2.980	132.6	0.26	0	3220	[14,20]
HFC-236fa	$CF_3CH_2CF_3$	124.92	3.200	\	\	0	6300	[17,21]
HFC-236ea	CF_2CHFCF_3	139.29	3.501	\	\	0	710	[17,20]
HFC-245fa	$CF_3CH_2CHF_2$	154.35	3.651	\	\	0	820	[21–23]
HFC-365mfc	$CF_3CH_2CF_2CH_3$	204.55	3.489	\	1.70	0	840	[24]
HFC-32	CH_2F_2	78.11	5.777	390.5	0.0043	0	675	[9,14–16,18,25]
HFC-23	CHF_3	25.85	4.815	240.0	0.10	0	11700	[18,25]

140 kJ mol^{-1} near the freezing point. The upper quadruple point Q_2, for L_g–L_w–H–V four-phase equilibrium, was tested at 283.19 K/ 0.416 MPa for HFC-134a hydrate, 283.95 K/0.930 MPa for HFC-125 hydrate, 283.33 K/0.838 MPa for HFC-143a hydrate. It is noticeable that, as long as one of the guest substances is in the gaseous state, the possible maximum of the hydrate formation temperature is T_{Q_2}. In order to utilize a fluid as the heat reservoir to which the heat released by the hydrate formation is discharged, T_{Q_2} is required to exceed the temperature of the fluid by several degrees [10]. More properties of refrigerant gases are listed in Table 3. Besides, HFCs hydrates that have potential to be PCMs for cold storage are: HFC-236ca, HFC-236cb, HFC-245ca, HFC-245cb, HFC-245ea, HFC-245eb, HFC-254ca, HFC-254cb, HFC-254ea, HFC-254eb, HFC-254fa and HFC-254fb.

2.2. CO_2 clathrate hydrate

Environmental issues related to the emission of greenhouse gases pose a great concern for refrigeration industry [26]. The utilization of CO_2 clathrate hydrate for cold storage is considered capable of achieving a high storage density, owing to the high dissociation enthalpy and large uptake efficiency of CO_2 in a limited hydrate volume, as well as relieving greenhouse effect problems by means of CO_2 recovery.

CO_2 molecules can form the sI clathrate hydrate and preferably fit in the $5^{12}6^2$ cages [27]. The clathrate has a critical temperature of 283.05 K and a critical pressure of 4.44 MPa [28]. By Differential Thermal Analysis (DTA) and Differential Scanning Calorimetry (DSC) methods, CO_2 hydrate was tested to offer a dissociation enthalpy of 501–507 kJ kg^{-1} [26]. Thus CO_2 slurry appears obvious advantages over many other types of slurry, such as ice (334 kJ kg^{-1}) and TBAB (200 kJ kg^{-1}). It was reported that when the global CO_2 mole fraction was 2.88 mol% and the temperature was 276.24 K, the hydrate fraction in the slurry was 2.8 vol% and the available enthalpy was up to 1.15×10^4 kJ m^{-3}(water) [29]. Therefore, CO_2 hydrate slurry is considered as a promising alternative of multiphase secondary refrigerant.

The general structure of CO_2 hydrate equilibrium data testing system is shown in Fig. 1 [30–36]. The system is mainly composed of three sections: a hydrate formation reactor cell, a gas supplying system and a measuring system. The reactor, which consists of an adiabatic cylindrical vessel, is installed on a magnetic stirrer with an agitator rotating within the liquid. The reactor is heated and cooled by an aqueous solution circulation into the jacket from a cryostat, and is linked to a gas storage vessel with a pressure reducing valve that maintains a constant pressure. The pressure in the reactor is measured by a pressure transducer while the temperature is measured by a probe inserted into the liquid.

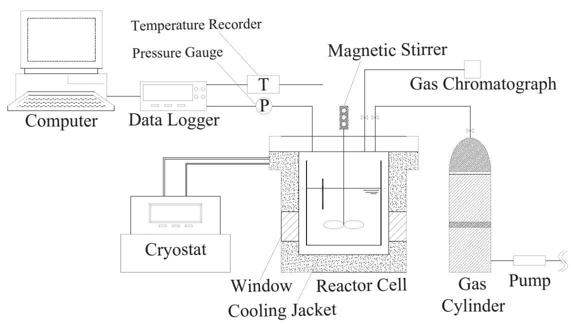


Fig. 1. Schematic of apparatus for measuring CO_2 clathrate hydrate equilibrium data.

CO_2 hydrate formation is widely examined from a chemical kinetics perspective. Jerbi et al. [37] investigated CO_2 hydrate formation kinetics in a semi-batch stirred tank in the aim of designing a circulation loop with heat exchangers for secondary refrigeration applications. They found that the hydrate growth was 1.45×10^{-3}%(hydrate)$\cdot$s^{-1} for a stirring velocity about 450 rpm. For an isothermal circulation loop, the kinetic rate varied from 5.45×10^{-3}%(hydrate)$\cdot$s^{-1} and 8.37×10^{-3}%(hydrate)$\cdot$s^{-1}, with and without additives respectively, for their dispersive and promoter properties. Yang et al. [38,39] built an engineering test module to examine the effects of gas carrier, fluid velocity, slurry concentration and temperature on the heat transfer and kinetics of CO_2 hydrate formation. The system (Fig. 2), was mainly composed of a gas delivery system, a CO_2-saturated and raw water delivery system, a continuous flow reactor, a chiller, and a data acquisition system, etc. It was found that when the flow pattern was maintained in annular flow region, hydrate formation rates were as high as 0.45 s^{-1} under favorable conditions. However, as the flow pattern changed to slug or plug flow, the apparent rate constants decreased significantly (in the worst case falling to <0.01 s^{-1}), underscoring the importance of good inter-phase mixing. With vigorous mixing, hydrate formation kinetics were favorable and the formation became heat transfer limited.

2.3. Hydrocarbon clathrate hydrates

Hydrocarbon gases can form sI, sII and sH hydrates. Small gas molecules such as CH_4 and C_2H_6 can be encaged in lattice cavities of sI hydrates; larger gas molecules such as C_3H_8 and C_4H_{10} can be encaged in lattice cavities of sII hydrates. Structures of hydrocarbon clathrate hydrates are summarized in Table 4 [40].

A number of experiments have been carried out with respect to the kinetics of hydrocarbon clathrate hydrates. According to the work of Bergeron et al. [41], the average reaction rate constant of

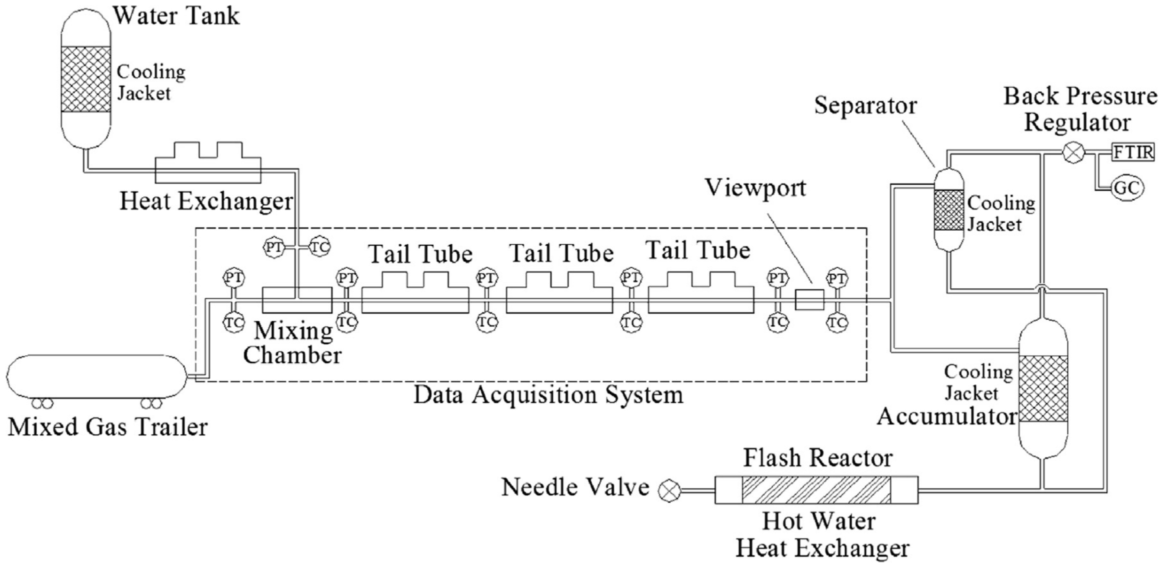


Fig. 2. Schematic diagram of the engineering test module system.

Table 4
Hydrate structures of hydrocarbon gases.

Structure of clathrate hydrate	Guest gas			
sI	Methane	Ethane		Methane + ethane
sII	Propane	Butane	Methane + propane	Methane + n-butane
sH	Methane + methylcyclopentane	Methane + n-pentane	Neohexane	Isopentane

CH_4 hydrate formation was around $8.3 \pm 0.5 \times 10^{-8}$ m s^{-1} with an average temperature of 275.1 K, and $61.5 \pm 4.8 \times 10^{-8}$ m s^{-1} with an average temperature of 279.1 K. The reaction rate constant was found to increase with the increase of temperature, with an activation energy of 323 kJ mol^{-1}. An intrinsic kinetic model for the formation of CH_4 and C_2H_6 hydrates was proposed by Englezos et al. [42], verified with experiments obtained in a semi-batch stirred tank. The formation rate was tested to be proportional to the difference in the fugacity of the dissolved gas and the three-phase equilibrium fugacity. This difference defined the driving force which incorporated the pressure effects. Moridis et al. [43] estimated the thermal properties and kinetic parameters of hydration reaction in porous media by means of simulation. It was shown that the intrinsic rate constant of the CH_4 hydrate dissociation reaction was 1.78×10^6 kg m^{-2} Pa^{-1} s^{-1} with the activation energy of 8.97×10^4 J mol^{-1}. Comparison with the results from pure CH_4 hydrate samples provided a measure of the effect of the porous medium on the kinetic reaction. It was also tested that the dissociation enthalpy of CH_4, C_2H_6, C_3H_8 and i-C_4H_{10} are 56.9, 71.1, 126.0, 130.4 kJ mol^{-1} [44]. The liquid–hydrate–vapor (L_w–H–V) phase equilibrium data of hydrocarbon gases are detailed in Table 5.

2.4. Multi-component clathrate hydrates

Single clathrate hydrates sometimes cannot meet all the conditions of a certain cold storage system. Accordingly, multi-component clathrate hydrates are proposed to improve global properties by complementary features of each component.

2.4.1. Multi-component system of refrigerant clathrate hydrates

Multi-component clathrate hydrates are potential to maintain the equilibrium pressures by adjusting the proportion of components. From Akiya et al. [59], the critical dissociation temperature and critical dissociation pressure of HFC-32 + HFC-125 mixtures with the HFC-32 fraction of 0, 52.49 and 100 wt% were 284.39 K/0.944 MPa, 291.55 K/1.429 MPa and 294.09 K/1.484 MPa, with the enthalpy of 135.0, 78.5 and 71.6 kJ mol^{-1}, respectively. Kobayashi et al. [15] measured the vapor–liquid equilibrium data for pure, binary and ternary systems containing HFC-32, HFC-125 and HFC-134a. As was calculated, COP for this system was higher than that for HCFC-22, resulting in about 15% energy-saving, when the mole fraction of HFC-32 and HFC-125 are 0.485 and 0.250, respectively. Lim et al. [60] used hydrocarbon gases to form hydrate with refrigerant gases. At 273.15 K, the equilibrium pressure of the propane + HFC-227ea system increased from 0.195 to 0.476 MP; while at 283.15 K, the equilibrium pressure increased from 0.280 to 0.632 MPa with the mole fraction of propane ranging from 0 to 100%. Besides these, HFC-134a/HCFC-141b [61], HFC-32/HFC-143a/HFC-134a [62], and HFC-134a/cyclopentane [63] were also estimated practicable for cold storage applications. Properties of some comprehensively used multi-component refrigerant gases are listed in Table 6. According to the advantage complementary principle, some refrigerant gas pairs that might be able to form feasible PCMs were proposed by Li et al. [12]: HFC-365mfc + HFC-134a, HFC-365mfc + HFC-152a, HFC-365mfc + HFC-227ea, HFC-236ea + HFC-134a, HFC-236ea + HFC-152a, HFC-236ea + HFC-227ea, HFC-245fa + HFC-134a, HFC-245fa + HFC-152a, HFC-245fa + HFC-227ea, HFC-236ea + HFC-134a, HFC-236ea + HFC-152a, HFC-236ea + HFC-227ea, cyclopentane + HFC-227ea and cyclopentane + HFC-152a.

2.4.2. Multi-component system of hydrocarbon clathrate hydrates

Phase equilibrium data of binary hydrocarbon clathrate hydrate systems, such as CH_4 + C_2H_6, CH_4 + C_3H_8 and CH_4 + i-C_4H_{10} were reported [45,47]. It was studied by Thakore et al. [64] that the presence of C_3H_8 and i-C_4H_{10} could largely bring down the equilibrium pressure of CH_4 hydrate from 3.370 to 0.278 MPa and from 3.099 to 0.128 MPa, respectively (Fig. 3). The equilibrium pressure of C_3H_8 + i-C_4H_{10} hydrates varied with a little change

Table 5
L_w–H–V phase equilibrium data of hydrocarbon clathrate hydrates.

Hydrocarbon gas	Molecular formula	Critical temperature[28] (K)	Critical pressure [28] (MPa)	Equilibrium temperature (K)	Corresponding equilibrium pressure (MPa)	Re
Methane	CH_4	\	\	273.7–285.9	2.77–9.78	[45]
				274.25–285.78	2.92–9.54	[46]
				285.7–301.6	9.62–68.09	[47]
				290.2–320.1	15.9–397.0	[48]
				305.08–320.54	98–493	[49]
Ethane	C_2H_6	287.85	3.35	273.7–286.5	0.51–2.73	[45]
				277.8–287.2	0.848–3.082	[50]
				278.8–288.2	0.95–3.36	[51]
				290–324	20–479	[52]
Propane	C_3H_8	278.85	0.545	273.2–278.0	0.165–0.472	[53]
				274.2–278.4	0.207–0.542	[54]
				276.77–278.55	0.368–0.547	[55]
Isobutane	i-C_4H_{10}	275.03	0.165	273.2–275.1	0.110–0.167	[56]
				273.2–275.0	0.115–0.169	[57]
Cyclopentane	C_5H_{10}	280.85	\	273.36–280.22	0.0069–0.0198	[58]

Table 6
Properties of multicomponent refrigerant gases.

HFCs	Components	Proportion	Critical temperature (°C)	Critical pressure (MPa)	ODP	GWP
R410a	R22/152a/124	53/13/34	107.3	4.61	0	1018
R410b	R22/152a/124	61/11/28	72.5	4.95	0	1221
R404a	R125/143a/134a	44/52/4	72.1	3.74	0	3922
R407a	R32/125/134a	20/40/40	75.7	4.24	0	2107
R407b	R32/125/134a	10/70/20	74.4	4.08	0	2804
R407c	R32/125/134a	23/25/52	86.7	4.62	0	1774
R408a	R125/143a/22	7/46/47	83.8	4.42	0	3036
R507a	R125/143a	50/50	70.9	3.79	0	3985

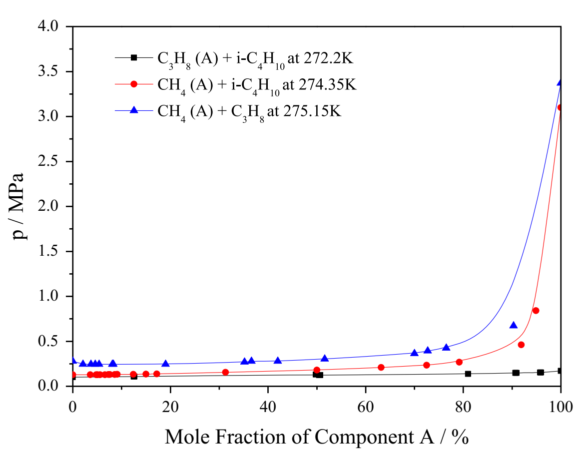


Fig. 3. Variation of the equilibrium pressure of binary hydrocarbon hydrates with mole fraction of components.

from 0.1013 MPa to 0.1713 MPa with proportion. The L_w–H–V phase equilibrium data of binary hydrocarbon clathrate hydrates are listed in Table 7. It is noticed that, in multi-component clathrate hydrate systems, the upper quadruple Q_2 evolves into a line caused by the fact that a single hydrocarbon is no longer presented, therefore a combination of hydrocarbon and water vapor pressures creates a broader phase equilibrium envelope. However, since the quadruple line has a gradient much larger than the L_w–H–V line, and the pressure on this line increases dramatically with an increase in temperature, the practical operations should better be implemented before T_{Q_2} is reached.

2.4.3. Multi-component system of CO_2/N_2 and hydrocarbon clathrate hydrates

Multi-component hydrates are sometimes prepared combining light alkane hydrocarbon gases with CO_2 or/and N_2. The formation of CH_4+CO_2 hydrate was observed by measuring the vapor-phase composition using gas chromatography and Raman spectroscopy by Uchida et al. [27]. It was indicated that the kinetics of the mixed clathrate hydrate was controlled by the competition of both molecules to be enclathrated into the hydrate cages. CH_4 molecules were preferentially crystallized in the early stages of hydrate formation when the initial concentration of CH_4 was much less than that of CO_2, thus pure CH_4 hydrates first formed. This phenomenon suggested that CH_4 molecules played important roles in hydrate formation. L_w–H–V phase equilibrium data of binary systems of hydrocarbon gases with CO_2 or N_2 are listed in Table 8. Phase equilibrium data of multi-component systems (with more than two guest gases) of hydrocarbon gases with CO_2 or/and N_2 are detailed in Table 9. The variations of the equilibrium pressure of C_3H_8, i-C_4H_{10} and n-C_4H_{10} combined with CO_2 at given temperatures are plotted in Fig. 4 [76]. It was showed that the global equilibrium pressure went up slowly with the increase of CO_2 proportion at low CO_2 mole fractions, while it went up sharply at high CO_2 mole fractions ($\geq$ 93%). However, there was a slight pressure drop in each line at very high CO_2 mole fractions ($\geq$ 98%).

3. Modification of clathrate hydrates

3.1. Decrease of equilibrium pressure

In many cases, clathrate hydrates cannot achieve equilibrium within the pressure range corresponding to adapted temperatures for cold storage systems. Taking CO_2 hydrate as an example, it manifests rigorous equilibrium conditions as is shown in Fig. 5 [1].

Tetra-n-butyl ammonium bromide (TBAB) has been subjected to the most intensive studies for modifying the phase equilibrium behavior of clathrate hydrates. TBAB in water can form a semi-clathrate hydrate in which TBAB molecules act as both the host

Table 7
L_w–H–V phase equilibrium data of binary hydrocarbon clathrate hydrates.

Gas composition	Mole fraction of component A (%)	Mole fraction of component B (%)	Equilibrium temperature (K)	Corresponding equilibrium pressure (MPa)	Re
Methane(A)+ethane(B)	1.60	98.40	283.9–287.8	1.810–3.080	[65]
	4.70	95.30	279.4–287.6	0.990–2.990	
	17.70	82.30	281.6–287.0	1.420–3.000	
	56.40	43.60	214.8–283.2	0.945–2.434	[45]
	90.40	9.60	274.8–283.2	1.524–3.965	
	98.80	1.20	274.8–280.4	2.861–5.088	
Methane(A)+propane(B)	23.75	76.25	274.9–281.4	0.263–0.830	[66]
	37.10	62.90	274.4–282.3	0.270–0.945	
	71.20	28.80	274.8–283.2	0.365–1.151	[45]
	88.30	11.70	274.8–283.2	0.552–1.558	
	99.00	1.00	274.8–283.1	1.627–4.358	
Methane(A)+isobutane(B)	36.40	63.60	273.8–276.9	0.159–0.284	[67]
	71.40	28.60	273.9–282.7	0.208–0.786	
	84.80	15.20	274.0–288.9	0.304–2.030	
	94.00	6.00	274.8–288.5	0.505–2.820	
	95.40	4.60	293.8–305.0	6.720–63.330	[47]
	98.90	1.10	274.8–277.6	1.324–1.841	[45]
	99.77	0.23	275.2–279.7	2.080–3.440	[67]
Methane(A)+n-butane(B)	94.18	5.82	277.99–281.43	2.050–3.290	[68]
	96.09	3.91	276.91–287.55	2.150–11.050	
	97.52	2.48	276.4–286.4	2.300–10.400	
	98.36	1.64	276.0–288.5	2.480–13.720	
Ethane(A)+propane(B)	28.00	72.00	276.5–277.9	0.460–0.660	[51]
	44.30	55.70	275.9–277.4	0.050–0.720	
	65.80	34.20	273.9–277.6	0.440–1.060	
	72.90	27.10	273.4–275.8	0.490–0.920	
	81.40	18.60	273.1–279.6	0.540–1.300	
	85.70	14.30	279.7–283.3	1.190–2.020	
Propane(A)+isobutane(B)	12.50	87.50	272.2	0.108	[69]
	49.80	50.20	272.2	0.130	
	95.90	4.10	272.2	0.153	
Propane(A)+n-butane(B)	72.50	27.50	273.2	0.244	[70]
	86.30	13.70	275.2	0.339	
	96.10	3.90	274.2	0.228	
Isobutane(A)+n-butane(B)	0.748	99.252	263.4–265.3	0.0732–0.0808	[71]
	0.77	99.23	261.1–267.3	0.0562–0.0688	
	0.835	99.165	264.3	0.0632	

and the guest. There are still small dodecahedral empty cages in this semi-clathrate hydrate, thus it is able to uptake, store and separate small gas molecules under certain thermal conditions [84,85]. Nguyen et al. [86] conducted experiments on CO_2-TBAB hydrate formation. The equilibrium pressure was lowered from 35 bar to 2.73 bar at 279.3 K with TBAB concentration of 0.29 mol %. As can be seen in Table 10, TBAB decreased the formation pressure by a factor of 10–50. Arjmandi et al. [87] measured phase boundaries of TBAB and different clathrate hydrates. The results showed that, in general, semi-clathrates of TBAB and guest gases were more stable than single clathrate hydrates at low-pressure conditions, and this stability increased with the increase of TBAB concentration. The dissociation conditions of these semi-clathrate hydrates are summarized in Table 11. However, this phenomenon would change at high-pressure conditions, especially for semi-clathrates formed with low TBAB concentrations. In the experiments conducted by Wang et al. [88], semi-clathrates were formed from gaseous mixtures of CO_2, H_2 and CO in TBAB solutions in an isochoric equilibrium cell with the TBAB concentrations of 0.05, 0.10 and 0.20 mol%. The equilibrium data for these hydrates are shown in Fig. 6. Meysel et al. [33] conducted experiments on semi-clathrates formation from CO_2 and N_2 (with the CO_2 fraction of 0.75, 0.50 and 0.20, respectively) in TBAB solutions with the TBAB concentration of 0.05, 0.10 and 0.20 mol%. The results are shown in Fig. 7, indicating a similar tendency of the effect of TBAB concentration on the global equilibrium pressure.

Small amounts of tetrahydrofuran (THF) can change the sI of CO_2 hydrate to sII, thus decreasing its equilibrium pressure. Martínez1 et al. [89] studied the equilibrium pressure of CO_2-THF hydrate with 10 wt% THF at 280 K and found that the equilibrium pressure reduced to 0.2 MPa, compared with 2.9 MPa of single CO_2 hydrate. Delahaye et al. [34] tested the formation conditions of CO_2–THF–water system using DTA and DSC. The results showed an average relative pressure decrease of 79% at a low initial concentration of THF (3.8 wt%). The formation pressure could be lowered to 0.038 MPa with the presence of 15 wt% THF. It is suggested that cyclopentane (CP) can also form sII clathrate hydrates with or without a help gas to fill small cavities and stabilize the structure [90]. Since CP only occupies large cavities, small gas molecules, such as H_2 and CO_2, can be more easily engaged in the small cavities. The dissociation temperature of H_2–CP hydrate under 2.7–11.1 MPa and CO_2–CP hydrates under 0.89–3.51 MPa were determined using a high-pressure Micro-DSC by Zhang et al. [91]. It was found that, the dissociation temperature of H_2–CP hydrate was higher than that of H_2–THF hydrate, but lower than that of H_2–TBAB hydrate; while the dissociation temperature of CO_2–CP hydrate was slightly higher than that of both CO_2–THF hydrate and CO_2–TBAB hydrate. Neopentane is also

Table 8
L_w–H–V phase equilibrium data of hydrocarbon gases and CO_2/N_2.

Gas composition	Mole fraction of component A (%)	Mole fraction of component B (%)	Equilibrium temperature (K)	Corresponding equilibrium pressure (MPa)	Re
Methane(A)+carbon dioxide (B)	92	8	283.2	6.80	[72]
	78	22	283.4	6.23	
	59	41	281.8	4.03	
	26	74	281.6	3.79	
	15	85	282.7	4.37	
	3.46	96.54	273.5–282.3	1.10–4.80	[73]
	31.7	68.3	280.3	3.24	[74]
	61.6	38.4		3.77	
	79.7	20.3		4.37	
	91.0	9.0		4.85	
Ethane(A)+carbon dioxide (B)	5.31	94.69	276.0–282.7	1.58–3.90	[73]
Propane(A)+carbon dioxide (B)	8	92	273.9–283.7	0.676–3.179	[75]
	25	75	280.2–283.8	0.979–1.917	
	60.0	40	274.8–279.7	0.324–0.793	
	83.0	17	278.2–279.1	0.503–0.641	
	90.1–1.5	9.9–98.5	273.7	0.2206–1.3583	[76]
	64.3–1.3	35.7–98.7	278.2	0.5516–2.2270	
	65.0–1.3	35.0–98.7	282.0	1.2483–3.69414	
Isobutane(A)+carbon dioxide (B)	79.3–0.7	20.7–99.3	273.7	0.1448–1.3238	
	46.0–1.0	54.0–99.0	277.6	0.4137–2.0822	
	20.9–2.1	79.1–97.9	280.9	0.8756–3.1716	
n-Butane(A)+carbon dioxide (B)	7.7–0.8	92.3–99.2	273.7	1.1379–1.3241	
	3.8–0.9	96.2–99.1	278.2	2.4000–2.3034	
Propane (A)+nitrogen (B)	6.18	93.82	274.5–289.2	1.72–13.71	[77]
	13	87	275.1–286.2	1.10–5.54	
	28.3	71.7	274.6–280.8	0.569–1.72	
	54.2	45.8	274.2–280.3	0.332–1.19	
	75	25	274.5–278.7	0.256–0.676	
Nitrogen (A)+carbon dioxide (B)	3.48	96.52	273.1–280.2	1.22–2.95	[73]
	9.01	90.99	273.4–279.1	1.37–3.09	
	82.39	17.61	272.85–280.55	7.240–14.220	[78]
	51.85	48.15	273.75–282.00	3.195–8.975	
	2.22	77.80	274.00–284.25	2.000–7.445	
	3.41	96.59	274.95–283.55	1.565–5.115	

recognized as a potential sII clathrate hydrate former. Dissociation data for CP and neopentane in their binaries and ternaries with CH_4 or/and N_2 was reported by Tohidi et al. [83]. The predicted hydrate dissociation conditions (Fig. 8), showed that CP and neopentane could lower the dissociation pressure to a larger extent than benzene and cyclohexane in their binaries with CH_4. The results of comparison with some other hydrate forming compounds indicated that CP was the strongest hydrate promoter, with neopentane in the second place. Besides, tetra-n-butylammonium chloride (TBACl), tetra-n-butylammonium nitrate ($TBANO_3$) and tetra-n-butylphosphonium bromide (TBPB) [92], cyclohexane, tetrahydropyran, 2-propanol [93,94], 1,4-dioxane and acetone [95], 3-methyl-1-butanol [35], methylcyclohexane (MCH) and cis-1,2-dimethylcyclohexane (cis-1,2-DMCH) [46] were also effective to moderate the equilibrium pressure of clathrate hydrates.

3.2. Increase of dissociation enthalpy

Dissociation enthalpy of clathrate hydrate relates directly to the capability of cooling releasing, thus is of great importance. The addition of THF can change the hydrate sI to sII and increased the amount of entrapped guest species, thus leading to enhanced hydrate stability and dissociation enthalpy. Delahaye et al. [34] found that the dissociation enthalpy of CO_2–THF systems were two times higher than that of single CO_2 hydrate. The enthalpy of the binary system was tested as 147.4 kJ mol^{-1} at 278.7 K with 10.16 wt% THF, compared with that of the pure CO_2 hydrate of 70.8 kJ mol^{-1} at 278.7 K. Depending on the concentration of CO_2 and THF, the dissociation enthalpy of mixed hydrates was found to be in the region of 112.37–152.27 kJ mol^{-1} [96]. Enthalpies for pure and mixed CO_2 and N_2 gases, with or without THF as an additive, were measured by Kang et al. [78], as can be seen in Table 12. For $G\cdot nH_2O$ hydrates, n stands for the number of water molecules in the unit cell and G stands for the pure guest gas; for $xCO_2\cdot yN_2\cdot 46H_2O$ hydrates, x and y are the calculated number of CO_2 and N_2 molecules, respectively, in sI; and for $xCO_2\cdot yN_2\cdot z\mathrm{THF}\cdot 136H_2O$ hydrates, x, y and z stands for the calculated number of CO_2, N_2 and THF molecules, respectively, in sII. In the work of Mayoufi et al. [92], DSC measurements of dissociation enthalpies of CO_2 hydrates with TBACl, $TBANO_3$ and TBPB were conducted. The CO_2–TBPB hydrate presented the highest dissociation enthalpy (Fig. 9). It was noticed that the fusion heat of mixed hydrates increased significantly with the increase of CO_2 pressure, which could be explained by the fact that TBACl, $TBANO_3$ and TBPB could also accommodate CO_2 in semi-clathrate structures and stabilize the structures, thus resulting in a lift in the dissociation enthalpy. Under pressures of 1–2 MPa, the dissociation enthalpy of CO_2–TBPB hydrate was even higher than that of CO_2–TBAB hydrate [97–99]. SH hydrates can store the largest amount of small guest gas principally because the ratio of small to large cages is 5:1, compared to 2:1 for sII and 1:3 for sI [100]. Nakamura et al. [46] found the addition of MCH and cis-1,2-DMCH can change the structure of CH_4 hydrates to sH, which not only increased the enthalpy but also reduced the hydrate formation pressure. The

Table 9
L_w–H–V phase equilibrium data of multicomponent hydrocarbon clathrate hydrates.

mol% of CH_4	mol% of C_2H_6	mol% of C_3H_8	mol% of i-C_4H_{10}	mol% of n-C_4H_{10}	mol% of i-C_5H_{12}	mol% of n-C_5H_{12}	mol% of C_6H_{14}	mol% of CO_2	mol% of N_2	Equilibrium temperature (K)	Corresponding equilibrium pressure (MPa)	Re
97.25	1.42	1.08	\	\	\	\	\	\	\	273.5–281.9	0.92–2.67	[79]
86.41	6.47	3.57	0.99	1.14	\	0.78	\	\	0.64	278.8–298.3	1.255–27.32	[80]
93.20	4.25	1.61	\	\	\	\	\	0.51	0.43	277.7–293.3	1.600–14.13	
88.36	6.82	2.54	0.38	0.89	\	1.01	\	\	\	276.8–293.2	1.207–12.00	
65.4	12.7	10.3	\	3.7	\	\	\	0.20	7.7	274.8–294.0	0.627–8.536	[45]
87.9	4.4	4.9	\	1.5	\	\	\	0.20	1.1	273.7–286.5	0.600–2.861	
78.4	6.0	3.6	\	2.4	\	\	\	0.20	9.4	273.7–283.2	0.724–2.213	
79.4	5.8	3.6	\	1.4	\	\	\	0.30	9.5	273.7–282.1	0.752–2.096	
91.0	3.2	2.0	\	3.1	\	\	\	0.40	0.3	273.7–292.7	0.765–9.391	
90.8	3.0	2.1	\	3.2	\	\	\		1.0	273.7–291.5	0.758–7.729	
75.2	5.9	3.3	\	1.1	\	\	\	0.20	14.3	274.2–282.1	0.758–2.131	
88.5	4.3	2.0	\	1.7	\	\	\		3.4	273.7–280.4	0.793–1.813	
90.6	3.8	1.5	\	2.0	\	\	\	0.9	1.2	273.7–290.9	0.883–8.384	
67.4	3.7	1.9	\	1.2	\	\	\	0.8	25.0	274.3–286.0	1.069–4.592	
96.5	0.9	1.8	\	\	\	\	\	0.6	0.2	273.7–289.8	1.262–10.439	
73.29	6.70	3.90	0.36	0.55	\	0.20	\	\	15.0	281.6–290.9	1.765–5.833	[81]
79.64	9.38	3.22	0.18	0.58	\	0.15	0.05	\	6.8	283.3–291.0	2.186–5.661	
72.78	14.50	7.63	\	2.65	\	0.63	0.11	\	1.70	288.75	4.207	[82]
67.69	13.50	14.10	\	2.45	\	0.58	0.10	\	1.58	289.85		
62.49	12.47	20.62	\	2.26	\	0.58	0.11	\	1.47	289.85		
76.62	11.99	6.91	1.82	2.66	\	\	\	\		273.7–282.0	0.4966–1.4138	[76]
52.55	8.12	4.74	1.31	1.88	\	\	\	31.40			0.5931–1.6828	
24.42	3.99	3.07	0.75	0.92	\	\	\	66.85			0.7586–2.2276	
12.38	1.96	1.66	0.37	0.48	\	\	\	83.15			1.3655–3.5103	
7.86	1.13	0.86	0.20	0.33	\	\	\	89.62			1.3379–3.4690	
85.24	7.68	3.31	1.19	0.85	0.30	0.31	\	0.22	0.90	279.1–294.8	1.317–11.769	[83]

mol% stands for mole fraction.

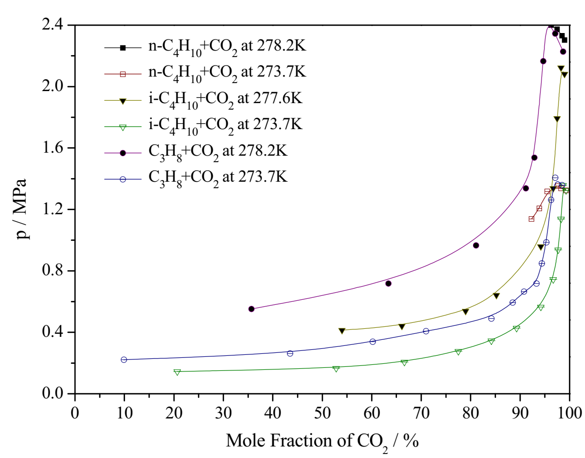


Fig. 4. Variation of the equilibrium pressure of binary clathrate hydrates of CO_2 and hydrocarbon gas with CO_2 mole fraction.

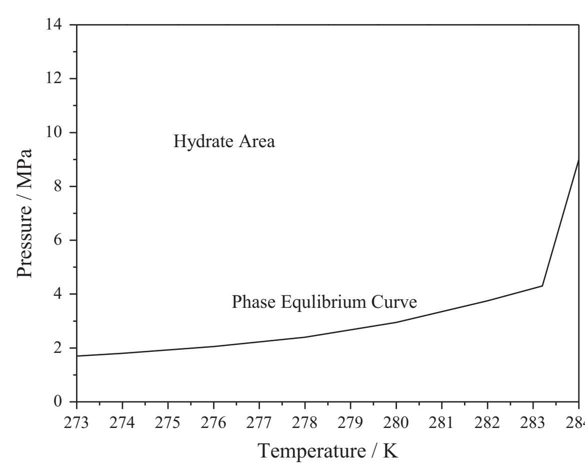


Fig. 5. Phase diagram of CO_2 clathrate hydrate.

enthalpy of CH_4–MCH hydrate was 374.1 kJ mol^{-1} at 274.09 K, and that of CH_4-cis-1,2-DMCH hydrate was 382.7 kJ mol^{-1} at 274.18 K.

3.3. *Acceleration of formation process*

Fast hydrate formation plays a critical role in efficient energy-saving considering cooling charging and discharging. However, the clathrate hydrate formation is a complex reaction kinetics problem in a multi-element and multi-phase heat flow system with irregular phase transition behavior and anomalous transient state. Clathrate hydrates generally form in the interface between two phases, and their further growth requires water or gas diffusing through the hydrate region, thus the crystallization would be

Table 10
Equilibrium pressure of CO_2 hydrate with and without TBAB.

TBAB (mol%)	*T* (K)	*P* (bar)	$P_{without\ TBAB}$ (bar)
0.29	279.3	2.73	35
	282	6.4	36.9
	284	8.4	143.6
0.61	286.1	10.7	270
	286.2	11.2	372
3.6	290.9	33.2	1220
9.4	284	8.15	143.6
	285	9.86	243

Table 11
Measured dissociation conditions of gas-TBAB clathrate hydrates.

Guest gas	Concentration of TBAB	T (K) (±0.2 K)	P (MPa)
Hydrogen	0.10	280.15	4.233
		281.45	9.639
	0.43	286.05	3.600
		286.25	5.226
Methane	0.05	287.15	4.688
		288.65	7.040
	0.10	287.15	2.413
		289.15	4.482
		290.65	6.757
	0.20	287.65	1.421
		290.15	3.310
		291.65	5.276
		293.35	8.028
	0.30	291.05	3.283
		292.65	5.110
		294.25	8.103
Nitrogen	0.10	285.15	4.688
		288.15	10.945
Carbon dioxide	0.10	285.55	1.400
		287.35	2.320
		289.25	4.090
	0.427	287.25	1.248
		288.75	1.793
		290.15	2.896
		291.15	3.517
Natural gas (87.32%methane+5.67% ethane+1.68%propane+0.23%2-methyl propane+0.40%n-butane+0.10%2-methyl butane+3.24% nitrogen+1.36%carbon dioxide)	0.05	280.35	0.979
		282.35	2.068
		283.55	2.854
		284.55	3.482
		286.95	5.419
		290.95	9.515
	0.10	283.15	1.145
		284.15	1.720
		286.97	3.694
		289.05	5.812
	0.43	286.15	0.828
		290.65	4.972
		292.45	7.966

time-consuming. The formation process of CO_2 hydrate is reported to be 100 min by Fournaison et al. [26] and 2 h by Delahaye et al. [101], and CH_4 hydrate formation is about three times longer than CO_2 hydrate formation [102]. For the purpose of accelerating clathrate hydrate formation, promoters such as mechanical agitation, magnetic interference, additives and structural optimization of the reactor are extensively proposed.

3.3.1. Mechanical agitation and magnetic interference

Xie et al. [103] compared three mechanical hydration enhancement methods. It was found that all characteristics were superior in the way of continuous mechanic blending method (with the total cold storage amount of 27.2 MJ and the average hydrate growth velocity of 0.5876 kg min^{-1}). However, the most energy was also consumed under continuous mechanical blending, and after a long time operation all connecting components in the system trended to loosen. According to Linga et al. [104] who obtained significant gas uptake and separation efficiency at lab-scale by stirring with a gas-inducing mechanical agitation system, hydrate crystallization must be carried out without mechanical agitation if hydrates are to be used commercially. That is, for safety and economic reasons, it would be better to work in quiescent conditions during hydrate formation. It was found that ultrasound could greatly improve gas–liquid mass transfer, especially below gas induction speed. This improvement was boosted by pressure. In typical conditions of organic synthesis: 323 K, 1100 rpm, 10 bar, the gas–liquid mass transfer coefficient in liquid phase was multiplied by 11 with ultrasound (20 kHz/62.6 W) [105]. Liu et al. [106] verified that ultrasonic wave had an impact on hydrate formation, and the range of ultrasonic wave power that was advantageous to promote the hydrate formation was 58–1000 W.

3.3.2. Additives

Surfactants, such as sodium dodecyl sulfate (SDS), sodium tetradecyl sulfate (STS) and sodium hexadecyl sulfate (SHS), cetyl trimethyl ammonium bromide (CTAB), dodecyl trimethyl ammonium bromide (DTAB), dodecyl trimethyl ammonium chloride (DTAC), linear alkyl benzene sulfonate (LABS), dodecylbenzene sulfonic acid (DBSA), sodium dodecyl benzene sulfonate (SDBS), ethoxylated nonylphenol (ENP), Tween and Span20, can provide nucleus and help to break through the metastability, thus are feasible for shortening the induction time.

The effects of three anionic surfactants, SDS, STS and SHS, on CH_4 hydrate formation were tested by Okutani et al. [107] in an unstirred chamber. In each experimental operation, hydrate formation continued for a limited time and then practically ceased, leaving only a small proportion (15% or less) of the aqueous solution unconverted into hydrate crystals. The variations in the time-averaged rate of hydrate formation were 7.0 h for SDS at 2000 ppm, 6.4 h for STS at 100 ppm, and 8.2 h for SHS at 100 ppm. It was reported that the addition of CTAB (100 ppm) to the water shortened the hydrate pressure decay halftime to 45 min, showing that the process could be catalyzed. Such catalysts could specifically enhance the building of the hydrate structures of CO_2 [108]. Besides, the effect of SDS, LABS, CTAB and ENP on the formation and dissociation of CH_4 hydrate have been investigated, with each tested with 3 concentrations (300, 500 and 1000 ppm) [109]. The effect of anionic surfactants DBSA and SDBS; cationic surfactants CTAB and DTAB; and non-ionic surfactants alkylpolyglucoside (APG), TritonX-100 (TX100), and dodecyl polysaccharide glycoside (DPG) on CH_4, C_2H_6 and C_3H_8 hydrate formation were studied by ZareNezhad et al. [110]. Li et al. [111] estimated the effects of DTAC in 0.29 mol% TBAB aqueous solution on the induction time of CO_2 hydrate formation. In another work of Li et al. [32], the effect of 0.29 mol% TBAB solution in conjunction with CP on hydrate-based CO_2 capture were investigated. More than 80 mol% of the amount of gas consumed were obtained within 400 s at 274.65–277.65 K and 2.5–4.5 MPa.

Structural revulsant, such as silver iodide and potassium oxalate monohydrate, is another kind of promoter which is used as the template agent. Porous medium, such as glass powder, silica gel, molecular sieve, poly HIPE, dry water and dry gel, can also accelerate the hydrate formation by promoting hydrate formation through the enhancement of mass transfer [112]. In addition, nanoparticles can be used to promote heat transfer between the gas and water, thus speeding up the growth of hydrate [113].

3.3.3. Structural optimization of the reactor

Formation process can also be accelerated by modifying the structure of the reactor. Okutani et al. [107] examined the promotion of CH_4 hydrate formation with the aid of a water-cooled cold plate, a steel-made flat-plate-type heat sink, vertically dipped into the aqueous phase across the gas/liquid interface. The increase in CH_4 uptake volume relative to its level in the absence of the cold plate was of a factor of 1.73. This factor exceeded that for the increase in the total surface area, 1.51, and that for the increase in the total horizontal perimeter, 1.62. Hydrate formation in a fixed bed column was conducted by Linga et al. [114], showing that the rate of hydrate formation was significantly greater and thereby resulted in a higher percent of water conversion of hydrate in

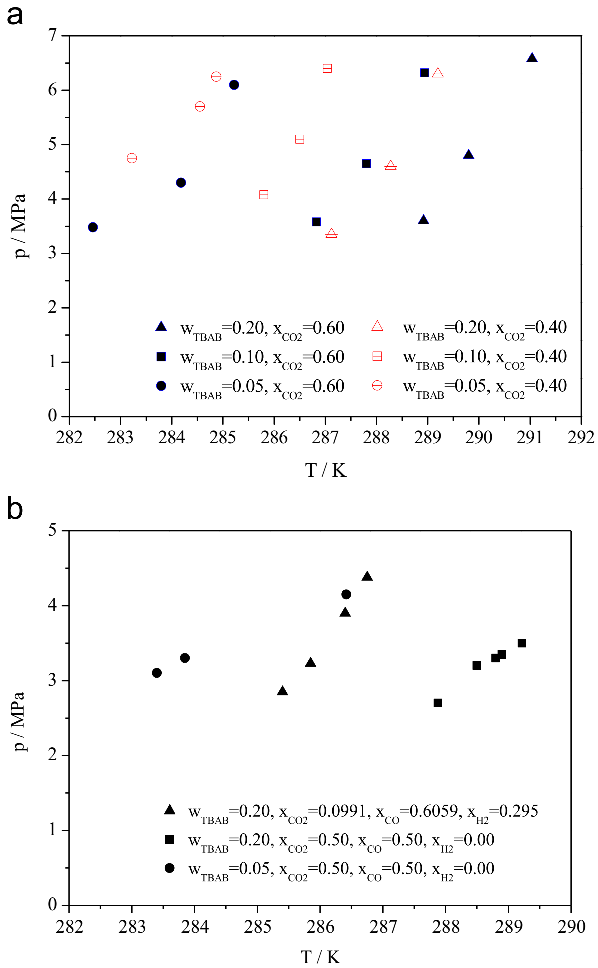


Fig. 6. Three-phase equilibrium conditions for hydrates formation from CO_2+CO+H_2 in TBAB aqueous solutions. (a) Binary mixture of CO_2 + H_2 and (b) Ternary mixture of CO_2 + CO + H_2.

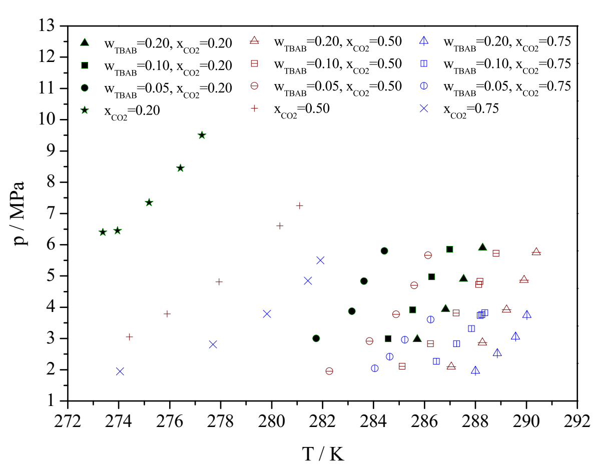


Fig. 7. Three-phase equilibrium conditions for hydrates formation from CO_2+N_2 in TBAB aqueous solutions.

lesser reaction time. For instance at about 3 h, the gas uptake in a stirred bed was about 0.019 mol(gas)·mol^{-1}(water), whereas that in the case of the fixed bed reactor was 0.083 mol(gas)·mol^{-1} (water). Li et al. [115,116] presented the favorable effects on the nucleation and growth of HCFC-141b clathrate hydrate in a static water column of adding an iron rod. The iron rod, combined with proper surfactant, effectively induced phase permeation between

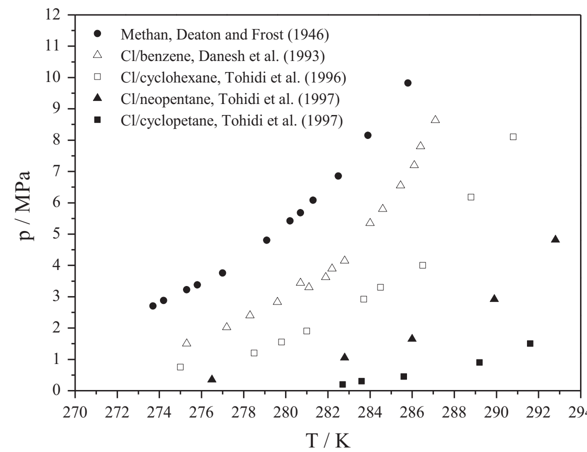


Fig. 8. Hydrate phase boundary for CH_4 and its binaries with heavy hydrate formers.

Table 12
Enthalpies of dissociation for pure and mixed CO_2 and N_2 gases with or without THF.

Guest gases	Dissociation enthalpy (kJ mol^{-1})	Hydrate composition
CO_2	65.22 ± 1.03	n=7.23
N_2	65.81 ± 1.04	n=5.94
0.17 CO_2+0.83 N_2	64.59 ± 1.02	x=5.43, y=1.89
0.70 CO_2+0.30 N_2	63.41 ± 1.00	x=7.08, y=0.25
0.17 CO_2+0.83 N_2+0.01THF+0.99H_2O	109.01 ± 1.72	x=2.96, y=9.47, z=11.39
0.17 CO_2+0.83 N_2+0.03THF+0.97H_2O	118.94 ± 1.87	x=2.35, y=7.42, z=12.53
0.70 CO_2+0.30 N_2+0.01THF+0.99H_2O	107.18 ± 1.69	x=9.97, y=2.58, z=10.94
0.70 CO_2+0.30 N_2+0.03THF+0.97H_2O	113.66 ± 1.79	x=8.11, y=2.19, z=13.16

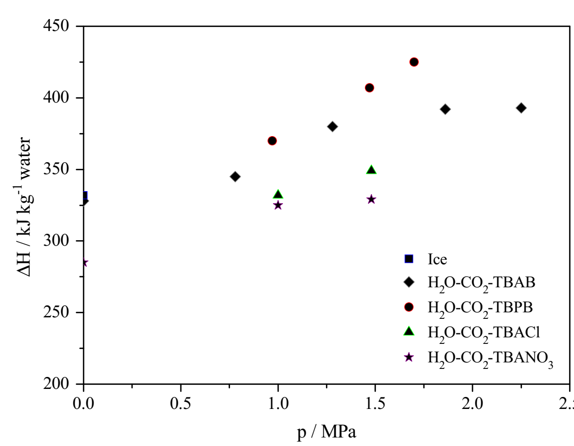


Fig. 9. Enthalpy of CO_2 hydrate with different additives under different pressures.

water and refrigerants, the hydrate formers, which were immiscible in general, thus considerably reducing the induction time for nucleation and promoting hydrate growth. When the temperature was 274.15–279.15 K, the hydrate nucleation happened in 3–30 min and the hydrate formation was completed in 1.5–8 h. In addition, the size of pressure vessel has an effect on the formation of clathrate hydrates. By McCallum et al. [117], the induction time of hydrate nucleation appeared to be greatly reduced by using a 72 L vessel which established the pressures and temperatures

required for CH_4 and CO_2 hydrate stability compared with a 450 mL Parr vessel.

3.4. Decrease of supercooling extent

The difference between critical dissociation temperature and hydrate reaction temperature is defined as supercooling extent, which, if occurs during clathrate hydrate formation, would lower the efficiency of a chiller. Thus, to minimize supercooling extent of clathrate hydrates imposes great importance on the performance of air conditioning systems.

It is feasible to decrease the supercooling extent by adding reasonable proportions of additives. According to Isobe et al. [118], the magnitude of supercooling required for the inception of HFC-134a hydrate was reduced moderately by adding alumina or zinc powder to the water phase in which HFC-134a was to be vaporized. An even larger reduction in supercooling can be achieved by adding a non-ionic surfactant. Besides, calcium hypochlorite can boost rapid crystal nucleus formation, and is a versatile cleaning chemical to clear away impurities and a strong oxidizer that can break down and destroy organic debris from adsorbing on the surface of the crystal nucleus or the growing crystal. Benzenesulfonic acid sodium salt can decrease the surface tension of water, decrease the diameter of bubbles and increase the rising frequency of bubbles, thereby decrease the resistance of mass transfer between gas and water molecules. Also, it makes the liquid emulsify into tiny liquid drops, thus the effective interface area between the two phases can be increased and great deal of hydrate nuclei is produced. Bi et al. [119] demonstrated a decrease in supercooling from 2.33 to 1.55 °C by adding benzenesulfonic acid sodium salt of 0.03%. The drawback of adding a surfactant is an increase in the effective specific volume of the resultant clathrate hydrate, calling for a larger space for storing a specified mass [118].

Although a larger flow rate can enhance the convection heat transfer between PCM and the secondary refrigerant, it can also cause a negligible temperature rise of PCM resulting in an increase in supercooling extent. The influence of flow rate of the reactor on supercooling extent was investigated by Bi et al. [120], presenting that when the flow rate was lower than $450\,l\,h^{-1}$, the supercooling extent decreased quickly with the increase of the flow rate to a minimum of 1.97 °C; while when the flow rate was larger than $450\,l\,h^{-1}$, the supercooling extent increased slowly with the increase of the flow rate. This optimized value of flow rate is practicable for the minimization of supercooling extent of clathrate hydrates.

3.5. Enhancement of gas phase solubility

Gas solubility has a rather large influence on the equilibrium pressures of some clathrate hydrates, such as H_2S and CO_2, because the solubility of these gases in water is quite high even at low pressures. The influence of gas solubility on the equilibrium pressures of CH_4 and N_2 is also important because of their high equilibrium pressures. The root mean square deviation on the calculation of the dissociation pressures for CH_4 with and without solubility along the L_w–H–V line is respectively 2.63% and 4.97% [121]. The solubilities of some hydrocarbon gases are listed in Table 13.

Temperature and pressure are two important factors on gas solubility. Hashemi et al. [122] carried out predictions using Henry's law to estimate the solubility of CO_2. Under a pressure of 2 MPa, the solubility of CO_2 rose from 0.0150 mol% at 274.0 K to a peak of 0.0174 mol% at 277.5 K, and then dropped linearly back to 0.0150 mol% at 285.0 K. The CO_2 solubility in pure water in the presence of CO_2 clathrate hydrate was measured at temperatures of 273–284 K and pressures from 2 to 6 MPa. It was found that the solubility increases with increasing temperature in the hydrate formation region; while in the absence of clathrate hydrate, the gas solubility increases with decreasing temperature. The amount of gas dissolved in liquid in equilibrium with clathrate hydrates was 0.0163 mol% at 274.25 K and 0.0281 mol% at 282.95 K with the pressure maintained at 6 MPa [123]. Thereby, the solubility of guest gas should be taken into consideration while determining the hydrate formation temperatures and pressures. In addition, co-solvents, such as dissolved propylene glycol (PPG) and polyethylene glycols (PEG), are also resorted to for increasing gas solubility [124,125]. However, how co-solvents affect the crystallization process of clathrate hydrates, especially at high concentrations, is still unknown.

4. Clathrate hydrates for cold storage air conditioning applications

4.1. Clathrate hydrate based cold storage air conditioning systems

Generally, clathrate hydrate based cold storage system can be classified into direct contact type and indirect contact type. Direct contact cold storage systems has no intermediate heat exchanger, thus manifests higher heat transfer efficiency and lower initial cost. However, it faces difficulties in oil return of the compressor. In contrast, although the indirect contact system with intermediate heat exchangers has a relatively higher facility cost, it can be operated under more practical conditions and is more potential to be applied in large-scaled systems. The charging and discharging principle of a refrigerant clathrate hydrate based cold storage system is illustrated in Fig. 10 [11,126].

An observational study was carried out on clathrate hydrate formation in a cold storage tank incorporated into a vapor compression refrigerator loop by Mori et al. [127]. The working fluid, R12, flowed into the cold storage tank (Fig. 11) and evaporates, resulting in the cooling of the fluids and the formation of R12 hydrate. The hydrate appeared in two forms, making up separate layers in tank: one in the form of slurry particles sedimented at the bottom and the other in the form of a solidified foam floating on the free surface of the water phase. The hydrate layer built on the lower water/R12 liquid interface had the form of a dense slurry while a sufficient amount of liquid water still remained in the crystallizer to suspend the hydrate particles. This feature is favorable for dense cold storage in a limited volume.

Fig. 12 illustrates the conceptual design of a clathrate hydrate based refrigeration system contrived by Ogawa et al. [10]. The system mainly consists of (1) a compressor in which gas and water are mixed and compressed, (2) a hydrate forming reactor in which the hydrate is formed at a temperature exceeding that in the environment of the system, thereby releasing heat to the environment, (3) a slurry pump for conveying the hydrate slurry and

Table 13
Solubility of natural gas under standard conditions.

Guest Gas	CH_4	C_2H_6	C_3H_8	i-C_4H_{10}	n-C_4H_{10}	C_5H_{10}	N_2	CO_2
Solubility ($\times 10^{-3}$)/g(gas) · k g^{-1}(water)	2.48	3.10	2.73	1.69	2.17	3.32	1.19	60.8

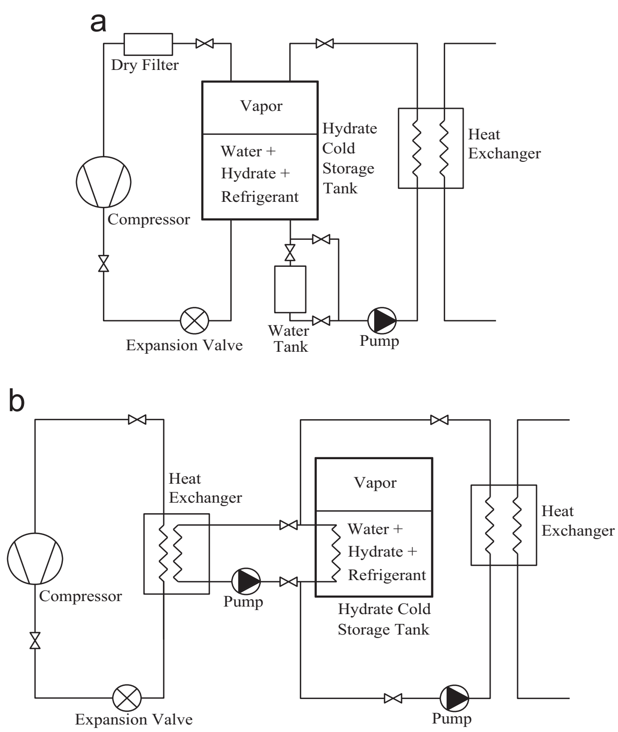


Fig. 10. Schematic diagram of direct contact and indirect contact hydrate based cold storage system.

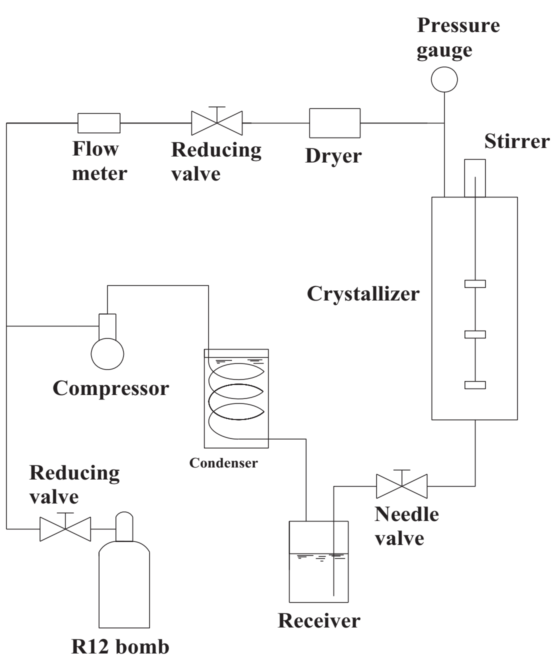


Fig. 11. Schematic diagram of a R12 hydrate based cold storage refrigeration system.

controlling the pressure difference between the two reactors, (4) the hydrate-dissociating reactor in which the hydrate is dissociated, thereby absorbing heat from a space to be cooled. The pair of HFC-32 and CP was selected as the working medium for simulation of this refrigeration system. The simulations revealed that, if the hydrate formation temperature and dissociating temperature were adjusted to 25.5 °C and 7.5 °C, respectively, the COP of the system should be as high as 8.0. This fact indicated that the

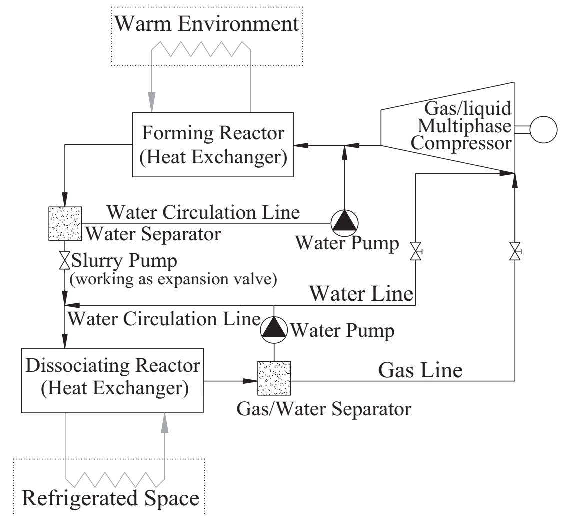


Fig. 12. Conceptual design of a clathrate hydrate based refrigeration system.

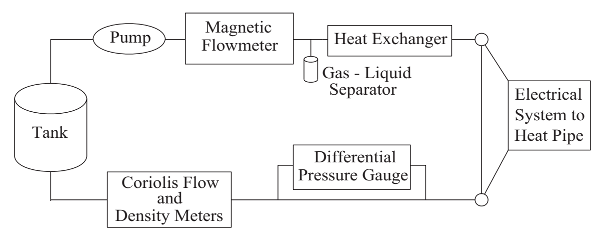


Fig. 13. Conceptual design of a refrigerant loop of CO_2 hydrate slurry.

hydrate-based refrigeration system could surpass conventional refrigeration systems in thermodynamic efficiency. Meanwhile, in a laboratory-scale hydrate-based refrigeration system, HCFC-22 was used as the guest substance with the temperature of 5 °C and the pressure of 0.4 MPa. The heat flow indicated that the system could be operated continuously over 2 h.

Jerbi et al. [128] presented a conceptual design of a refrigeration system in which CO_2 hydrate slurry was used as a two-phase secondary fluid, which allowed CO_2 hydrate slurry forming and dissociating continuously. The loop is shown in Fig. 13. The system was composed of two parts, one for the formation and storage of CO_2 hydrate slurry (the tank reactor) and another for its circulation and dissociation (the circulation loop). The tank reactor had a capacity of 25 L, which could resist a pressure about 4.5 MPa and provide a heat flux about 1–5 kW for a hydrate fraction between 10% and 30%. When the CO_2 hydrate flowed in the loop, the heat exchanger was chosen to allow the decomposition of the slurry and exchange the same heat flux as which was provided in the reactor.

4.2. *Improvement methods of charging and discharging performance*

Bi et al. [120] developed a HCFC-141b hydrate cold storage experimental system, including a cold storage tank and cold/hot reservoirs. The experimental results indicated that the cold storage effect of the system was better when the volumetric flow rate in the crystallizer was 150–450 l h^{-1} and the corresponding cooling rate was 0.055–0.105 °C min^{-1}, then the formation rate of HCFC-141b hydrate was 0.30–0.4 g s^{-1}, and the cooling energy stored was 2.9–4.0 MJ. Experimental research on the discharging process in a clathrate hydrate cold storage system was also performed by

Bi et al. [119,129]. In this system, the inner-heat exchanger/outer-crystallization technology and the integrated condenser/evaporator structure were adopted. Results showed that the instantaneous dissociation rate was close to twice as the corresponding instantaneous formation rate of gas-hydrate, and the cooling energy release rate was obviously higher than the storage rate, which was resulted from the temperature difference between the heat transfer medium and the clathrate hydrate.

Both the charging and the discharging process were dominated by heat transfer and mass transfer. However, as to the discharging process, the effect of the heat transfer was the main influencing factor [129]. Therefore, charging and discharging performance improvement may focus on heat and mass transfer enhancement. A novel small scale of clathrate hydrate cold storage apparatus, consisted of a storage tank, a refrigeration system and a cooling release system, was designed by Xie et al. [130]. The operating results showed that the cold storage performance could be improved greatly by adding a heat exchanger with vertical metal fins in the tank; SDS (the additive) with concentration of 0.04 wt% helped to improve the cold storage performance, with the total cold storage amount raised to 27.2 MJ, the average hydrate growth velocity up to 0.5876 kg min^{-1} and the Hydrate Packed Factor up to 49.7%. In addition, decreasing of the coolant temperature or increasing of the coolant flow rate could also make the amount of stored cooling increased [103]. HFC-134a clathrate hydrate, though has excellent phase change properties, it alone cannot be industrially used because the hydrate floating would cause the upper space in the storage tank to be filled and cause difficulties in charging and discharging. Wu et al. [131] developed a HFC-134a hydrate cold storage system with alcohol additives. The results showed that 1.34% n-butanol additive exhibited the best result which substantially accelerated the cold storage rate. The lumped hydrate density increased apparently comparing with pure HFC-134a hydrate, which eliminated the hydrate floating during the hydration process under certain additive concentration. It was indicated that the added alcohol was essential for a stable and smooth cold storage operation, and a cold storage tank with indirect-contact configuration was industrially applicable. The hydration characteristics of a quiescent reactor with inner-placed vertical heat transfer tube were theoretically studied. The reaction material was R141b water solution with 300 ppm sodium dodecyl sulfate. In this case, water can permeate into the guest phases along the surface of heat transfer tube, thus massive clathrate hydrate could grow steadily along the vertical heat transfer tube in guest phases without mechanic stirring. It was also revealed that the coolant temperature had great effects on the growth rate: the lower the coolant temperature, the quicker the clathrate hydrate grew.

Taking entropy generation minimization as optimization objective, the optimal control strategies of the clathrate hydrate cold storage system were determined by Bi et al. [132]. It was indicated that the entropy generation at the phase change stage occupied the most portions of the total entropy generation. The optimal operating characteristic of the clathrate hydrate cold storage system could be achieved by keeping the phase change rates uniform, which were regulated and controlled according to constant heat transfer rates in the charging and discharging processes. The minimum entropy generation in the optimal configuration decreased by 8.2% compared with normal situation, showing that the optimal control was effective to improve the performance of cold storage system.

4.3. Clathrate hydrate slurry

In order to be considered as a suitable secondary refrigerant, clathrate hydrate slurry should fulfill satisfying flowing conditions. Firstly, the pressure and temperature conditions should be adapted to the operating environment of air conditioning applications. Secondly, the fluid should contain a relatively large fraction of solid phase to supply enough cooling energy and stable temperature level. Thirdly, the flowing conditions should be supportive to preserve efficient heat transfer. Clathrate hydrate slurries could be rheologically characterized by its apparent viscosity, which strongly depends on the mass fraction and the organization of solid particles in the liquid phase related to the nucleation, growth, shape, size distribution, agglomeration, etc.

According to the behavior index n and the yield stress $\tau_\circ$, fluids can be classified into five patterns [101]: Newtonian Fluid when $n=1$ and $\tau_\circ=0$, and then $\tau_w=\mu\dot{\gamma}_w$; Bingham Fluid when $n=1$ and $\tau_\circ>0$, then $\tau_w-\tau_\circ=\kappa\dot{\gamma}_w$; Pseudoplastic Fluid when $0<n<1$ and $\tau_\circ=0$, then $\tau_w=\kappa\dot{\gamma}_w^n$; Dilatant Fluid when $n>1$ and $\tau_\circ=0$, then $\tau_w=\kappa\dot{\gamma}_w^n$; Herschel–Bulkley Fluid when $0<n<1$ and $\tau_\circ\neq 0$, then $\tau_w-\tau_\circ=\kappa\dot{\gamma}_w^n$. τ_w is the shear stress, $\dot{\gamma}_w$ is the shear rate, μ is the dynamic viscosity, and κ is the viscosity coefficient. Using the Ostwald viscometer method, τ_w, $\dot{\gamma}_w$ and n can be calculated from

$$\tau_w=\frac{D\Delta P}{4L} \tag{1}$$

$$\dot{\gamma}_w=\left(\frac{8u}{D}\right)\left(\frac{3n+1}{4n}\right) \tag{2}$$

$$n=\frac{d\ ln\,(D\Delta P/4L)}{d\ ln(8u/D)} \tag{3}$$

where D is the pipe diameter, m; L is the pipe length, m; ΔP is the pressure drop, Pa; u is the fluid velocity, m s^{-1}. The rheological equation and apparent viscosity data of different hydrate slurries from numerous academics are summarized in Table 14.

5. Promising features of clathrate hydrates as cold storage media

5.1. Self-preservation effect

Clathrate hydrates of some gases exist at temperatures below the ice melting point outside their stable region. This anomalous behavior is known as the self-preservation phenomenon, which is of considerable scientific interest since it would make it possible to store cooling under ice point, and boost practical application for natural clathrate hydrate storage and transportation [140]. For instance, CH_4 hydrate can be stored at atmospheric pressure below the melting point of ice, even though this temperature is well outside the zone of thermodynamic stability of the hydrate and allows dissociation [141]. Melnikov et al. [142] observed that hydrates could exist in a metastable state without visible dissociation for a long time within the pressure–temperature area bounded by the I–H–V equilibrium line, the supercooled L_w–H–V metastable equilibrium line and the isotherm $T=253$ K for CH_4 hydrates or $T=263$ K for C_3H_8 hydrates. The long life time of hydrates in a metastable state suggested the presence of a significant energy barrier (the activation energy) for ice nucleation on the hydrate surface, and the ice-shielding model was suggested to explain the self-preservation phenomenon. Additionally, the role of the supercooled water in hydrate self-preservation has been discussed. The self-preservation effect of clathrate hydrates has spawned much research, but the mechanism is still not well understood. For example, one remaining puzzle is that $CH_4+C_2H_6$, a mixed clathrate hydrate of sII, does not show preservation behavior comparable to CH_4 hydrate, whereas its dissociation pressure is lower than that of CH_4 hydrate at the same temperature [4].

Table 14
Rheological equation and apparent viscosity data of different hydrate slurries.

Slurries	Rheological equation at different hydrate concentration	Apparent viscosity (mPa s)	Re
CO_2 hydrate slurry	4–20 vol% Herschel–Bulkley fluid	4.5–34.92 (γ=500 s^{-1})	[101]
	4–10 vol% Dilatant fluid	3.8–42.2 (γ=400 s^{-1})	[133]
	10 Vol% Bingham Fluid		
	10–20 vol% Pseudoplastic fluid		
CH_4 hydrate slurry	Bingham fluid	1–3.5	[134]
R141b hydrate slurry	Dilatant fluid	1.1–1.7 (γ=400 s^{-1})	[135]
TBAB hydrate slurry	Pseudoplastic fluid	50–148 (γ=400 s^{-1})	[136]
	43–55 wt% Bingham fluid	\	[137]
	12–70 wt% Pseudoplastic fluid	3.5–1000 (γ=1–1000 s^{-1})	[138]
TBAF hydrate slurry	0–42 wt% Pseudoplastic fluid	10–750 (γ=1–1000 s^{-1})	
TBPB hydrate slurry	0–28.2 vol% Pseudoplastic fluid	4–41	[139]
	9.5–33 wt% Pseudoplastic fluid	\	[92]

γ stands for shear rate.

5.2. Memory effect

Academics found that the induction time of hydrate formation using the water that dissociated from previous hydrates was much shorter than that of hydrate formation using unused water, while the reformed hydrates will still melt at the same dissociation temperature. This phenomenon was termed as memory effect [143,144]. It is suggested that for various species of clathrate in gas–liquid systems, such as CO_2/water and hydrocarbon gas/water, memory effect possesses a modified structure which allows easier hydrate re-formation [145]. Once applied memory effect in air conditioning systems, the hydrate would undergo a continuously charging and discharging, thus the induction time could be largely reduced. Wu et al. [146] has carried out experiments in a pressure cell. In this study, from the first test to the fourth test, the induction time of the system was 129.50, 73.28, 37.85 and 16.93 min, respectively. However, when the dissociation temperature was higher than 25 °C, the memory effect vanished. The memory effect for cyclopentane hydrate formation has been investigated by Sefidroodi et al. [147], revealing that provided the superheating above the equilibrium temperature (7.7 °C) was no more than 2–3 °C, the hydrates was obtained much faster during cooling to 0.0 °C than formed for the first time. Sun et al. [148] studied the clathrate hydrate formation in two systems: one with Tween-40 at 1×10^{-3} mol L^{-1} and another with Tween-40 at 2×10^{-3} mol L^{-1}. It was concluded that the induction time was shortened by 10–20 times in the experimental system containing residual structures. With respect to the mechanism of the memory effect, it has been reported [149] that the hydrate was observed to melt from the periphery outwards leaving a hydrate core. It was assumed that the residual structure of hydrate dissociation, as the source of the memory effect, provides a site for mass transfer between host and guest molecules. Therefore, a driving force is created between the residual structures and its surrounding bulk phase to promote the hydrate nucleation.

5.3. Gas conversion

Gas conversion from a CH_4 clathrate hydrate to a CO_2 clathrate hydrate would be advantageous for CH_4 hydrate dissociation and CO_2 hydrates formation. It is assumed that, if CH_4 and CO_2 hydrates are together utilized in a cold storage system, the gas conversion process would make it possible to charge and discharge cooling in two steps at two different temperatures, thus fulfill energy gradient utilization for a certain cold storage application and cooling demand.

For the replacement mechanism, it is assumed that the CO_2–CH_4 replacement chiefly includes two parts: CH_4 hydrate dissociation and mixed hydrate re-formation from the dissociated water and free water. The conversion of CH_4 hydrate into CO_2 hydrate may thus, in principle, be a solid state transformation in hydrate phase. In the re-formed hydrate, CO_2 molecules mainly occupy large cages while CH_4 molecules mainly occupy small cages. Pure CH_4 and pure CO_2, as well as mixtures of CH_4 and CO_2, would form sI hydrate [150,151]. Qi et al. [152] showed that, without the hydrate dissociation, CH_4 molecules were not easily released for the clathrate cages and CO_2 molecules could not penetrate into the interior cages of the hydrate because of the barrier of the cage walls constructed by hydrogen-bonding network. From the work of Lee et al. [153], CH_4–CO_2 conversion phenomenon occurring in clathrate hydrates was examined through thermodynamic equilibrium studies and a ^{13}C NMR spectroscopic analysis. The experimental results showed that approximately 67% of CH_4 was recoverable after replacement by CO_2. The corresponding chemical formula for the mixed clathrate hydrate after CO_2 replacement was $5.03CO_2\cdot2.51CH_4\cdot46H_2O$. From an energy perspective, the activation energy for CO_2 hydrate formation (73.3 kJ mol^{-1}) was found to be much larger than that for CH_4 hydrate dissociation (14.5 kJ mol^{-1}), and the solid diffusion manifested a large activation energy. In fact, several experimental investigations showed that the activation energy for diffusion of the H_2O molecule in the bulk ice was in the range of 52–70 kJ mol^{-1} [154,155]. Wang et al. [156] measured the kinetics of the CH_4 hydrate formation from neutron diffraction and reported that the activation energy for the diffusion in hydrate phase was 61.5 kJ mol^{-1}.

With respect to the influencing factors on the conversion, it was found that the replacement rate and the mole fraction of CH_4 in gas phase increased with the increase of initial CO_2 mole fraction, the decrease of system pressure, and the increase of diffusion coefficient of CH_4 in hydrate [151]. Compared with injecting gaseous CO_2 method, liquid CO_2 injection was also benefit for the recovery of CH_4 from hydrate. The replacement percent of CH_4 hydrate decreased with the increase of hydrate saturation, but increased with the increase of water saturation [157].

5.4. Hydrate structure transformation

Guest gases in sII and sH hydrates are generally more stable than those in sI hydrates, which means a greater amount of energy is required to dissociate the hydrate structure, and hence more enthalpy of dissociation is produced. It was reported that sII hydrates commonly have a dissociation enthalpy approximately two times higher than that of sI hydrates [39]. Therefore, it is

promising to improve the hydrate characteristics by structure transformation from sI to sII or sH.

The existence of different sized cages in the sI and sII hydrates is involved in the structural transition between sI and sII, which is prompted by the compositional changes of guest mixtures. In an investigation of Fleyfel et al. [158], CO_2 was able to form sII. It was obtained that the sI hydrate was formed when with ethylene oxide, and CO_2 occupied both the small and the large cavities. When CO_2 hydrate was grown epitaxially to THF hydrate, sII was formed and CO_2 occupied the small cavities only [159]. In pure CH_4 hydrate, high-pressure studies revealed that upon compression, sI CH_4 hydrate transforms to sII at 100 MPa, and then to the sH at 600 MPa. Thus under increasing pressure, the clathrate found more efficient ways to pack its guest molecules into cages [160]. Clathrate hydrates formed from binary gas mixtures of CH_4 and other small lipophilic molecules changed from sI to sII and back depending on the concentration of CH_4 in the mixtures, although CH_4 and the other gases each formed the sI hydrates [161]. CH_4 and N_2 are found to be the main components in natural gas. Pure CH_4 and N_2 formed sI and sII hydrate, respectively, while the structure of the mixed clathrate hydrate was found to largely depend on their relative gas composition. Lee et al. [162] investigated phase and structural behavior according to the composition of CH_4+N_2 gas mixture. It was showed that the clathrate hydrate changed its structure from sI to sII between 25.24 and 28.51 mol% CH_4 concentration. In addition, natural gas mixtures may form sII hydrate if the gas content of C_3H_8 and C_4H_{10} is sufficiently high. SII hydrate has a ratio of 2:1 of small to large cavities and will benefit from the extra stabilization of the larger cavities by hydrocarbons up to butanes, or other organic or inorganic molecules of similar size [150]. The kinetics of sII clathrate hydrates formed from pure C_3H_8 and a mixture of C_3H_8 and C_2H_6 were investigated in a semi-batch stirred tank reactor with pure C_3H_8. The intrinsic rate constant for C_3H_8 hydrate was between 0.42 and 0.52 mol m^{-2} MPa^{-1} s^{-1}. The intrinsic rate constant for C_2H_6 in sII was subsequently regressed on the formation of hydrates formed from an equimolar mixture of C_3H_8 and C_2H_6, and it was found to be 0.0137 mol m^{-2} MPa^{-1} s^{-1} at 274 K/0.35 MPa, which was more than one order of magnitude smaller than that in sI hydrate [163].

6. Conclusions

Clathrate hydrates, if used as cold storage medium, have obvious advantages over water for the high cold storage density; over ice for the compatible phase change temperature; and over eutectic salts for the remarkable heat transfer properties and ageing resistance. For the purpose of evaluating and promoting the utilization of clathrate hydrates in cold storage air conditioning systems, a review of recent research progress concerning the characteristics of clathrate hydrates, optimization of clathrate hydrate properties, and clathrate hydrate based cold storage systems, is presented. Refrigerant clathrate hydrates, CO_2 clathrate hydrates, hydrocarbon clathrate hydrates and multi-component clathrate hydrates are introduced, and technologies to modify their phase change properties are discussed. Moreover, clathrate hydrates based cold storage air conditioning systems are evaluated, and the optimizing methods of the system performance are summarized. There still remain some topics to be investigated in future.

(1) It was concluded by many academics that multi-component clathrate hydrates were more competitive alternatives as PCMs than single clathrate hydrates. Therefore, more investigations concerning the formation and dissociation conditions, phase change behavior, and heat and mass transfer properties of multi-component clathrate hydrates are needed.
(2) The area of clathrate hydrate phase equilibrium has reached a high level of maturity; however, data for hydrate formation and dissociation in the presence of substances that alter the phase diagram are needed for cold storage and other particular applications [159].
(3) Additives are usually used to modify phase change properties of clathrate hydrates, such as to lower equilibrium pressure, to accelerate formation rate, and to increase phase change enthalpy. However, the effects of additives on the long-term use of clathrate hydrates as cold storage media are still unknown.
(4) Nano-particles are recently widely used to enhance heat transfer performance of PCMs. However, unlike clathrate hydrates, most PCMs charge and discharge cooling energy via solid–liquid phase change and are not much related to the vapor phase. The addition of nano-particles in clathrate hydrates and its effect on the L_w–H–V phase equilibrium is also a topic to be studied.
(5) Semi-clathrate hydrates that employ TBAB [164], TBAF [165,166], TBAC, TBPB, TBMAC [167], TBACl and $TBANO_3$ [92], are intensively proposed. It has been found that semi-clathrate structures are good for easier and faster formation of clathrate hydrate with larger phase change enthalpy, thus is worthy to be adopted to cooling applications.
(6) Although attention has been paid to the performance of clathrate hydrate based cold storage systems, the investigation methods are still limited to lab-scaled experiments. It is suggested that large-scaled clathrate hydrate based systems could be built by simulation, to study how clathrate hydrates act for cooling supply to buildings, in order to provide predictions and estimations for actual cold storage cases.
(7) Features of clathrate hydrates, namely the self-preservation effect, memory effect, gas conversion and hydrate structure transformation, are benefit for the utilization as cold storage media. Further study should be put onto the fundamental mechanisms of these features, as well as onto the ways to make use of these features in practical applications.

References

[1] Weijun Chen, Liu Ni, Xiao Chen, et al. Perspective of CO_2 hydrate slurry application in air conditioning system with cool storage. J Refrig 2012;33 (3):1–4 ([in Chinese]).
[2] Dendy Sloan E, Koh Carolyn A. Clathrate hydrates of natural gases. 3rd ed. FL, USA: CRC Press; 2007; 1.
[3] Carroll John. Natural gas hydrates – a guide for engineers. 2nd ed. MA, USA: Elsevier Science & Technology; 2009; 1.
[4] Takeya Satoshi, Ripmeester John A. Dissociation behavior of clathrate hydrates to ice and dependence on guest molecules. Angew Chem Int Ed Engl 2008;47(7):1276–9.
[5] Eslamimanesh Ali, Mohammadi Amir H, Richon Dominique. Thermodynamic model for predicting phase equilibria of simple clathrate hydrates of refrigerants. Chem Eng Sci 2011;66(21):5439–45.
[6] Hashimoto Shunsuke, Miyauchi Hiroshi, Inoue Yoshiro, et al. Thermodynamic and Raman Spectroscopic studies on difluoromethane (HFC-32)+water binary system. J Chem Eng Data 2010;55:2764–8.
[7] Hashimoto Shunsuke, Makino Takashi, Inoue Yoshiro, et al. Three-phase equilibrium relations and hydrate dissociation enthalpies for hydrofluorocarbon hydrate systems: HFC-134a, -125, and -143a hydrates. J Chem Eng Data 2010;55:4951–5.
[8] Wilson LC, Wilding WV, Wilson GM, et al. Thermophysical properties of HFC-125. Fluid Phase Equilib 1992;80:167–77.
[9] Higashi Y. Critical parameters for HFC134a, HFC32 and HFC125. Int J Refrig 1994;17(8):524–31.
[10] Ogawa Tomohiro, Ito Tomonari, Watanabe Kenji, et al. Development of a novel hydrate-based refrigeration system: a preliminary overview. Appl Therm Eng 2006;26:2157–67.
[11] Jinggui Chen, Shuanshi Fan, Deqing Liang. Progress of cool storage technology with gas hydrate. Chem Ind Eng Prog 2003;22(9):942–6 ([in Chinese]).
[12] Gang Li, Yingming Xie, Daoping Liu. New type gas hydrate cool-storage media. J Refrig 2008;29(3):18–23 ([in Chinese]).

[13] Lim JS, Park JY, Lee BG, et al. Phase equilibria of 1,1,1-trifluoroethane (HFC-143a)+ 1,1,1,2-tetrafluoroethane (HFC-134a), and +1,1-difluoroethane (HFC-152a) at 273.15, 293.15, 303.15, and 313.15 K. Fluid Phase Equilib 2002;193:29–39.
[14] Park JY, Lim JS, Lee BG, et al. High pressure vapor-liquid equilibria of binary mixtures composed of HFC-32, 125, 134a, 143a, 152a, 227ea and R600a (isobutane). Fluid Phase Equilib 2002;194–197:981–93.
[15] Kobayashi Masanao, Nishiumi Hideo. Vapor–liquid equilibria for the pure, binary and ternary systems containing HFC32, HFC125 and HFC134a. Fluid Phase Equilib 1998;144(1–2):191–202.
[16] Park JY, Lim JS, Lee BG, et al. Phase equilibria of CFC alternative refrigerant mixtures: 1,1,1,2,3,3,3-heptafluoropropane (HFC-227ea)+difluoromethane (HFC-32),+1,1,1,2-tetrafluoroethane (HFC-134a), and +1,1-difluoroethane (HFC-152a). Int J Thermophys 2001;22(3):901–17.
[17] Gierczak Tomasz, Talukdar Ranajit K, Burkholder James B, et al. Atmospheric fate and greenhouse warming potentials of HFC 236fa and HFC 236ea. J Geophys Res 1996;101(D8):12,905–11.
[18] Lim JS, Park JY, Lee BG. Vapor–liquid equilibria of CFC alternative refrigerant mixtures: trifluoromethane (HFC-23)+difluoromethane (HFC-32), trifluoromethane (HFC-23)+ pentafluoroethane (HFC-125), and pentafluoroethane (HFC-125)+ 1,1-difluoroethane (HFC-152a). Int J Thermophys 2000;21(6) 1339–49.
[19] Na Liu, Xuyang Wang, Junming Li. Experimental investigation on heat transfer of R152a during condensation in a circular microchannel. J Eng Thermophys 2013;34(3):517–21 ([in Chinese]).
[20] Uchida Yuko, Yasumoto Masahiko, Yamada Yasufu, et al. Critical properties of four HFE+HFC binary systems: trifluoromethoxymethane (HFE-143m)+ pentafluoroethane (HFC-125),+1,1,1,2-tetrafluoroethane (HFC-134a),+1,1,1, 2,3,3,3-heptafluoropropane (HFC-227ea), and +1,1,1,2,3,3-hexafluoropropane (HFC-236ea). J Chem Eng Data 2004;49:1615–21.
[21] Hong Lin, Yuanyuan Duan, Zhongwei Wang. Surface tension measurements of 1,1,3,3-pentafluoropropane (HFC-245fa) and 1,1,1,3,3,3-hexafluoropropane (HFC-236fa) from 254 to 333 K. Fluid Phase Equilib 2003;214(1):79–86.
[22] Zipfel L, Krucke W, Borner K, et al. HFC-365mfc and HFC-245fa progress in application of new HFC blowing agents. J Cell Plast 1998;34:511–25.
[23] Ning Li, Xin Zhang, Hao Bai, et al. The study on thermal performance of power generation system using organic rankine cycle and reheating cycle system. Ind Heat 2012;41(2):44–7 ([in Chinese]).
[24] Bobbo Sergio, Scattolini Mauro, Fedele Laura, et al. Compressed liquid densities and saturated liquid densities of HFC-365mfc. Fluid Phase Equilib 2004;222–223:291–6.
[25] Lisal M, Vacek V. Effective potentials for liquid simulation of the alternative refrigerants HFC-32: CH2F2 and HFC-23: CHF_3. Fluid Phase Equilib 1996;118: 61–76.
[26] Laurence Fournaison, Anthony Delahaye, Imen Chatti, et al. CO_2 hydrates in refrigeration processes. Ind Eng Chem Res 2004;43:6521–6.
[27] Uchida Tsutomu, Ikeda Ikuko Y, Takeya Satoshi, et al. Kinetics and stability of CH_4–CO_2 mixed gas hydrates during formation and long-term storage. Chem Phys Chem 2005;6:646–54.
[28] Dendy Sloan E, Koh Carolyn A. Clathrate hydrates of natural gases. 3rd ed. FL, USA: CRC Press; 2007; 78.
[29] Sandrine Marinhas, Anthony Delahaye, Laurence Fournaison, et al. Modelling of the available latent heat of a CO_2 hydrate slurry in an experimental loop applied to secondary refrigeration. Chem Eng Process 2006;45:184–92.
[30] Torré Jean-Philippe, Dicharry Christophe, Ricaurte Marvin, et al. CO_2 capture by hydrate formation in quiescent conditions: in search of efficient kinetic additives. Energy Proc 2011;4:621–8.
[31] Belandria Veronica, Mohammadi Amir H, Richon Dominique, et al. Compositional analysis of the gas phase for the CO_2+N_2+tetra-n-butylammonium bromide aqueous solution systems under hydrate stability conditions. Chem Eng Sci 2012;84(24):40–7.
[32] Xiaosen Li, Chungang Xu, Zhaoyang Chen, et al. Hydrate-based precombustion carbon dioxide capture process in the system with tetra-n-butyl ammonium bromide solution in the presence of cyclopentane. Energy 2011;36:1394–403.
[33] Meysel Philipp, Oellrich Lothar, Bishnoi P Raj, et al. Experimental investigation of incipient equilibrium conditions for the formation of semi-clathrate hydrates from quaternary mixtures of (CO_2+N_2+TBAB$+H_2O$). J Chem Thermodyn 2011;43(10):1475–9.
[34] Anthony Delahaye, Laurence Fournaison, Sandrine Marinhas, et al. Effect of THF on equilibrium pressure and dissociation enthalpy of CO_2 hydrates applied to secondary refrigeration. Ind Eng Chem Res 2006;45:391–7.
[35] Joon Shin Hyung, Yun-Je Lee, Jun-Hyuck Im, et al. Thermodynamic stability, spectroscopic identification and cage occupation of binary CO_2 clathrate hydrates. Chem Eng Sci 2009;64:5125–30.
[36] Duc Nguyen Hong, Chauvy Fabien, Herri Jean-Michel. CO_2 capture by hydrate crystallization – a potential solution for gas emission of steelmaking industry. Energy Convers Manag 2007;48(4):1313–22.
[37] Jerbi S, Delahaye A, Fournaison L, et al. Characterization of CO_2 hydrate formation. In: Proceedings of 8th IIR conference on phase change materials and slurries for refrigeration and air conditioning. Karlsruhe, Germany; 2009.
[38] Dali Yang, Le Loan A, Martinez Ronald J, et al. Kinetics of CO_2 hydrate formation in a continuous flow reactor. Chem Eng J 2011;172:144–57.
[39] Dali Yang, Le Loan A, Martinez Ronald J, et al. Heat transfer during CO_2 hydrate formation in a continuous flow reactor. Energy Fuels 2008;22: 2649–59.
[40] Gang Li, Yingming Xie, Daoping Liu. Advances of gas hydrate cool storage media selection. J Refrig 2008;29(3):18–23 ([in Chinese]).
[41] Bergeron Sebastien, Beltrán Juan G, Servio Phillip. Reaction rate constant of methane clathrate formation. Fuel 2010;89(2):294–301.
[42] Englezos P, Kalogerakis N, Dholabhai PD, et al. Kinetics of formation of methane and ethane gas hydrates. Chem Eng Sci 1987;42:2647–58.
[43] Moridis GJ, Seol Y, Kneafsey TJ. Studies of reaction kinetics of methane hydrate dissociation in porous media. In: Proceedings of 5th international conference on gas hydrates. Trondheim, Norway; 2005.
[44] Sloan ED, Fleyfel F. Hydrate dissociation enthalpy and guest size. Fluid Phase Equilib 1992;76:123–40.
[45] Deaton WM, Frost EM. Gas hydrates and their relation to the operation of natural-gas pipe lines. US Bur Mines Monogr 1946;8:101.
[46] Nakamura Toshiyuki, Makino Takashi, Sugahara Takeshi, et al. Stability boundaries of gas hydrates helped by methane – structure-H hydrates of methylcyclohexane and cis-1,2-dimethylcyclohexane. Chem Eng Sci 2003;58 (2):269–73.
[47] Harry O, McLeod Jr O, Campbell John M. Natural gas hydrates at pressures to 10,000 psia. J Pet Technol 1961;13(6):590–4.
[48] Marshall Donald R, Saito Shozaburo, Kobayashi Riki. Hydrates at high pressures: part I. Methane–water, argon–water, and nitrogen–water systems. AIChE J 1964;10(2):202–5.
[49] Nakano Shinya, Moritoki Masato, Ohgaki Kazunari. High-pressure phase equilibrium and Raman microprobe spectroscopic studies on the methane hydrate system. J Chem Eng Data 1999;44(2):254–7.
[50] Avlonitis D. Multiphase equilibria in oil-water hydrate forming systems [M.S. thesis]. Scotland: Heriot-Watt University; 1988.
[51] Holder GD, Hand JH. Multiple-phase equilibria in hydrates from methane, ethane, propane and water mixtures. AIChE J 1982;28(3):440–7.
[52] Morita Kentaro, Nakano Shinya, Ohgaki Kazunari. Structure and stability of ethane hydrate crystal. Fluid Phase Equilib 2000;169:167–75.
[53] Miller B, Strong ER. Hydrate storage of natural gas. Am Gas Assoc Mon 1946;28(2):63.
[54] Kubota H, Shimizu K, Tanaka Y, et al. Thermodynamic properties of R13 ($CClF_3$), R23 (CHF_3), R152a ($C_2H_4F_2$), and propane hydrates for desalination of sea water. J Chem Eng Jpn 1984;17(4):423–9.
[55] Mooijer-van den Heuvel MM, Peters CJ, de Swaan Arons J. Gas hydrate phase equilibria for propane in the presence of additive components. Fluid Phase Equilib 2002;193(1–2):245–59.
[56] Schneider GR, Farrar J. Nucleation and growth of ice crystals. U.S. Department of Interior, Research Development. Report no. 292; 1968. p. 37.
[57] Rouherl Olivier S, Barduhn Allen J. Hydrates of iso- and normal butane and their mixtures. Desalination 1969;6(1):57–73.
[58] Fan SS, Liang DQ, Guo KH. Hydrate equilibrium conditions for cyclopentane and a quaternary cyclopentane-rich mixture. J Chem Eng Data 2001;46: 930–2.
[59] Akiya Takaji, Shimazaki Tomio, Oowa Masaru, et al. Phase equilibria of some alternative refrigerants hydrates and their mixtures using for cool storage materials. In: Proceedings of 32nd intersociety energy conversion engineering conference. Honolulu, Hawaii; 1997.
[60] Sung Lim Jong, Gimyeong Seong, Hee-Kook Roh, et al. Vapor–liquid equilibria for propane (R-290)+1,1,1,2,3,3,3-heptafluoropropane (HFC-227ea) at various temperatures. J Chem Eng Data 2007;52:2250–6.
[61] Kaihua Guo, Bifen Shu, Yi Zhang, et al. Phase-equilibrium properly of HFC134a/HCFC141b mixed gas hydrate. J Eng Thermophys 1998;19(4):480–3 ([in Chinese]).
[62] Huaixin Wang, Junying Sun, Li Fu, et al. Performance of HFC32/HFC143a/ HFC134a as a substitute for HCFC22 in air conditioning & direct cool storage cycle. J Eng Thermophys 2000;21(2):153–5 ([in Chinese]).
[63] Deqing Liang. The thermodynamic study on the phase equilibrium of new-type cool storage media refrigerant gas hydrates [PhD. thesis]. China: Shanghai Jiao Tong University; 2001.
[64] Thakore Jashwantsinh L, Holder Gerald D. Solid vapor azeotropes in hydrate-forming systems. Ind Eng Chem Res 1987;26(3):462–9.
[65] Holder GD, Grigoriou GC. Hydrate dissociation pressures of (methane+ethane+water) existence of a locus of minimum pressures. J Chem Thermodyn 1980;12(11):1093–104.
[66] Verma VK. Gas hydrate from liquid hydrocarbon–water system [PhD. thesis]. USA: University of Michigan; 1974.
[67] Wu Bing-Jing, Robinson Donald B, Ng Heng-Joo. Three- and four-phase hydrate forming conditions in methane+isobutane+water. J Chem Thermodyn 1976;8(5):461–9.
[68] Ng HJ, Robinson DB. The role of n-butane in hydrate formation. Chem Eng J 1976;22(4):656–61.
[69] Holder GD, Kamath VA. Hydrates of (methane+cis-2-butene) and (methane+trans-2-butene). J Chem Thermodyn 1984;16(4):399–400.
[70] Paranjpe SG, Patil SL, Kamath VA, et al. Hydrate equilibria for binary and ternary mixtures of methane, propane, isobutane, and n-Butane: effect of salinity. In: Proceedings of 62nd SPE annual conference. Dallas, USA; 1987.
[71] Godbole SP. Dissociation pressures of propane and I-butane hydrates below the ice point [M.S. thesis]. USA: University of Pittsburgh; 1981.
[72] Adisasmito Sanggono, Frank III Robert J, Dendy Sloan Jr. E. Hydrates of carbon dioxide and methane mixtures. J Chem Eng Data 1991;36(1):68–71.
[73] Shuanshi Fan, Tianmin Guo. Hydrate formation of CO_2-rich binary and quaternary gas mixtures in aqueous sodium chloride solutions. J Chem Eng Data 1999;44(4):829–32.

[74] Ohgaki A, Takano K, Sangawa H, et al. Methane exploitation by carbon dioxide from gas hydrates – phase equilibria for CO_2–CH_4 mixed hydrate system. J Chem Eng Jpn 1996;29(3):478–83.
[75] Robinson DB, Mehta BR. Hydrates in the propane–carbon dioxide–water system. J Can Pet Technol 1971;48:642–4.
[76] Sanggono Adisasmito, Dendy Jr. Sloan E. Hydrates of hydrocarbon gases containing carbon dioxide. J Chem Eng Data 1992;37(3):343–9.
[77] Ng Heng-Joo, Petrunia Jonathan P, Robinson Donald B. Experimental measurement and prediction of hydrate forming conditions in the nitrogen–propane–water system. Fluid Phase Equilib 1977-1978;1(4):283–91.
[78] Kang SP, Lee H, Ryu BJ. Enthalpies of dissociation of clathrate hydrates of carbon dioxide, nitrogen, (carbon dioxide+nitrogen), and (carbon dioxide+nitrogen+tetrahydrofuran). J Chem Thermodyn 2001;33(5):513–21.
[79] Donghai Mei, Jian Liao, Jitao Yang, et al. Hydrate formation of a synthetic natural gas mixture in aqueous solutions containing electrolyte, methanol, and (electrolyte+methanol). J Chem Eng Data 1998;43(2):178–82.
[80] Wilcox Willard I, Carson DB, Katz DL. Natural gas hydrates. Ind Eng Chem 1941;33(5):662–5.
[81] Kobayashi R, Withrow HJ, Williams GB, et al. Gas hydrate formation with brine and ethanol solutions. In: Proceedings of 13th annual convention. Tulsa, USA: Oklahoma Natural Gasoline Association of America; 1951.
[82] Lapin A, Cinnamon SJ. Problem of hydrate formation in natural gas systems. In: Proceedings of liquid natural gas: its production, handling, and use. London, Britain; 1969.
[83] Tohidi B, Danesh A, Todd AC, et al. Equilibrium data and thermodynamic modeling of cyclopentane and neopentane hydrates. Fluid Phase Equilib 1997;138:241–50.
[84] Zhang P, Ma ZW, Wang RZ. An overview of phase change material slurries: MPCS and CHS. Renew Sustain Energy Rev 2010;14(2):598–614.
[85] Gholinezhad Jebraeel, Chapoy Antonin, Tohidi Bahman. Separation and capture of carbon dioxide from CO_2/H_2 syngas mixture using semi-clathrate hydrates. Chem Eng Res Des 2011;89(9):1747–51.
[86] Duc Nguyen Hong, Chauvy Fabien, Herri Jean-Michel. CO_2 capture by hydrate crystallization – a potential solution for gas emission of steelmaking industry. Energy Convers Manag 2007;48(4):1313–22.
[87] Arjmandi Mosayyeb, Chapoy Antonin, Tohidi Bahman. Equilibrium data of hydrogen, methane, nitrogen, carbon dioxide, and natural gas in semi-clathrate hydrates of tetrabutyl ammonium bromide. J Chem Eng Data 2007;52:2153–8.
[88] Su Wang, Michael Danner, Thomas Kuchling, et al. Measurement of the three-phase (vapour+liquid+solid) equilibrium conditions of semi-clathrates formed from mixtures of CO_2, CO and H_2. J Chem Thermodyn 2013;56:149–52.
[89] Martínez1 MC, Dalmazzone D, Fürst W, et al. Thermodynamic properties of THF+CO_2 hydrates in relation with refrigeration applications. AIChE J 2008;54(4):1088–95.
[90] Ripmeester JA, Ratcliffe CI, McLaurin GE. The role of heavier hydrocarbons in hydrate formation. In: Proceedings of AIChE spring meeting – hydrates in the gas industry. Houston, USA; 1991.
[91] Zhang JS, Lee Jae W. Equilibrium of hydrogen+cyclopentane and carbon dioxide+cyclopentane binary hydrates. J Chem Eng Data 2009;54:659–61.
[92] Mayoufi N, Delahaye A, Fournaison L, et al. Characterization of CO_2 clathrate hydrate slurries for secondary refrigeration applications. In: Proceedings of 9th IIR conference on PCMs and slurries for refrigeration and air conditioning. Sofia, Bulgaria; 2010.
[93] Østergaard KK, Tohidi B, Anderson R, et al. Can 2-propanol form clathrate hydrates? Ind Eng Chem Res 2002;41:2064–8.
[94] Ohmura Ryo, Takeya Satoshi, Uchida Tsutomu, et al. Clathrate hydrate formed with methane and 2-propanol: confirmation of structure II hydrate formation. Ind Eng Chem Res 2004;43:4964–6.
[95] Eslamimanesh Ali, Gharagheizi Farhad, Illbeigi Mohammad, et al. Phase equilibrium modeling of clathrate hydrates of methane, carbon dioxide, nitrogen, and hydrogen+water soluble organic promoters using support vector machine algorithm. Fluid Phase Equilib 2012;316:34–45.
[96] Sabil Khalik M, Witkamp Geert-Jan, Peters Cor J. Estimations of enthalpies of dissociation of simple and mixed carbon dioxide hydrates from phase equilibrium data. Fluid Phase Equilib 2010;290:109–14.
[97] Deschamps J, Dalmazzone D. Dissociation enthalpies and phase equilibrium for TBAB semi-clathrate hydrates of N_2, CO_2, N_2+CO_2 and CH_4+CO_2. J Therm Anal Calorim 2009;98:113–8.
[98] Fan S, Li S, Wang J, et al. Efficient capture of CO_2 from simulated flue gas by formation of TBAB or TBAF semiclathrate hydrates. Energy Fuels 2009;23 (8):4202–8.
[99] Kamata Y, Yamakoshi Y, Ebinuma T, et al. Hydrogen sulfide separation using tetra-n-butyl ammonium bromide semi-clathrate (TBAB) hydrate. Energy Fuels 2005;19:1717–22.
[100] Khokhar AA, Gudmundsson JS, Sloan ED. Gas storage in structure H hydrates. Fluid Phase Equilib 1998;150–151:383–92.
[101] Anthony Delahaye, Laurence Fournaison, Sandrine Marinhas, et al. Rheological study of CO_2 hydrate slurry in a dynamic loop applied to secondary refrigeration. Chem Eng Sci 2008;63:3551–9.
[102] Yuanyuan He, Rudolph E Susanne J, Zitha Pacelli LJ, et al. Kinetics of CO_2 and methane hydrate formation: an experimental analysis in the bulk phase. Fuel 2011;90:272–9.
[103] Yingming Xie, Gang Li, Daoping Liu, et al. Experimental study on a small scale of gas hydrate cold storage apparatus. Appl Energy 2010;87:3340–6.
[104] Linga Praveen, Kumar Rajnish, Lee Ju Dong, et al. A new apparatus to enhance the rate of gas hydrate formation: application to capture of carbon dioxide. Int J Greenh Gas Control 2010;4(4):630–7.
[105] Laugier F, Andriantsiferana C, Wilhelm AM, et al. Ultrasound in gas-liquid systems: effects on solubility and mass transfer. Ultrason Sonochem 2008;15:965–72.
[106] Yonghong Liu, Kaihua Guo, Deqing Liang. Study on refrigerant hydrate crystallization process in the action of ultrasonic. J Eng Thermophys 2003;24(3):385–7 ([in Chinese]).
[107] Okutani Kazunori, Kuwabara Yui, Mori Yasuhiko H. Surfactant effects on hydrate formation in an unstirred gas/liquid system: An experimental study using methane and sodium alkyl sulfates. Chem Eng Sci 2008;63:183–94.
[108] van Denderen Mark, Ineke Erik, Golombok Michael. CO_2 removal from contaminated natural gas mixtures by hydrate formation. Ind Eng Chem Res 2009;48(12):5802–7.
[109] Ganji H, Manteghian M, Sadaghiani zadeh K, et al. Effect of different surfactants on methane hydrate formation rate, stability and storage capacity. Fuel 2007;86:434–41.
[110] ZareNezhad Bahman, Varaminian Farshad. A unified approach for description of gas hydrate formation kinetics in the presence of kinetic promoters in gas hydrate converters. Energy Convers Manag 2013;73:144–9.
[111] Xiaosen Li, Chungang Xu, Zhaoyang Chen, et al. Tetra-n-butyl ammonium bromide semi-clathrate hydrate process for post-combustion capture of carbon dioxide in the presence of dodecyl trimethyl ammonium chloride. Energy 2010;35:3902–8.
[112] Long F, Fan S, Wang Y, et al. Promoting effect of super absorbent polymer on hydrate formation. J Nat Gas Chem 2010;19(3):251–4.
[113] Jinping Li, Deqing Liang, Kaihua Guo, et al. Formation and dissociation of HFC134a gas hydrate in nano-copper suspension. Energy Convers Manag 2006;47(2):201–10.
[114] Linga Praveen, Daraboina Nagu, Ripmeester John A, et al. Enhanced rate of gas hydrate formation in a fixed bed column filled with sand compared to a stirred vessel. Chem Eng Sci 2012;68:617–23.
[115] Jinping Li, Kaihua Guo, Deqing Liang, et al. Experiments on fast nucleation and growth of HCFC141b gas hydrate in static water columns. Int J Refrig 2004;27:932–9.
[116] Jinping Li, Deqing Liang, Kaihua Guo, et al. The influence of additives and metal rods on the nucleation and growth of gas hydrates. J Colloid Interface Sci 2005;283:223–30.
[117] McCallum Scott D, Riestenberg David E, Zatsepina Olga Y, et al. Effect of pressure vessel size on the formation of gas hydrates. J Pet Sci Eng 2007;56:54–64.
[118] Isobe F, Mori YH. Formation of gas hydrate or ice by direct-contact evaporation of CFC alternatives. Int J Refrig 1992;15(3):137–42.
[119] Yuehong Bi, Tingwei Guo, Tingying Zhu, et al. Influences of additives on the gas hydrate cool storage process in a new gas hydrate cool storage system. Energy Convers Manag 2006;47:2974–82.
[120] Yuehong Bi, Tingwei Guo, Tingying Zhu, et al. Influence of volumetric-flow rate in the crystallizer on the gas-hydrate cool storage process in a new gas-hydrate cool-storage system. Appl Energy 2004;78:111–21.
[121] Lundgaard Lars, Mollerup Jorgen M. The influence of gas phase fugacity and solubility on correlation of gas-hydrate formation pressure. Fluid Phase Equilib 1991;70:199–213.
[122] Hashemi Shahrzad, Macchi Arturo, Bergeron Sebastien, et al. Prediction of methane and carbon dioxide solubility in water in the presence of hydrate. Fluid Phase Equilib 2006;246:131–6.
[123] Servio Phillip, Englezos Peter. Effect of temperature and pressure on the solubility of carbon dioxide in water in the presence of gas hydrate. Fluid Phase Equilib 2001;190:127–34.
[124] King Jr. AD. The Solubility of gases in aqueous solutions of poly (propylene glycol). J Colloid Interface Sci 2001;243:457–62.
[125] King Jr. AD. The Solubility of gases in aqueous solutions of polyethylene glycols. J Colloid Interface Sci 1991;144(2):579–85.
[126] Jingjing Wei, Yingming Xie, Daoping Liu. Applications of hydrate on cool storage and refrigeration (heat pump) system. J Refrig 2009;30(6):135–42 ([in Chinese]).
[127] Mori T, Mori YH. Characterization of gas hydrate formation in direct-contact cool storage process. Int J Refrig 1989;12(5):259–65.
[128] Jerbi S, Delahaye A, Fournaison L. Design of a new circulation loop and heat transfer of CO_2 hydrate slurry. In: Proceedings of 9th IIR conference on PCMs and slurries for refrigeration and air conditioning. Sofia, Bulgaria; 2010.
[129] Yuehong Bi, Tingwei Guo, Liang Zhang, et al. Experimental study on cool release process of gas-hydrate with additives. Energy Build 2009;41:120–4.
[130] Yingming Xie, Kaihua Guo, Deqing Liang, et al. Steady gas hydrate growth along vertical heat transfer tube without stirring. Chem Eng Sci 2005;60:777–86.
[131] Jianghong Wu, Shiping Wang. Research on cool storage and release characteristics of R134a gas hydrate with additive. Energ Build 2012;45:99–105.
[132] Yuehong Bi, Tingwei Guo, Liang Zhang, et al. Entropy generation minimization for charging and discharging processes in a gas-hydrate cool storage system. Appl Energy 2010;87:1149–57.
[133] Anthony Delahaye, Laurence Fournaison, Salem Jerbi, et al. Rheological properties of CO_2 hydrate slurry flow in the presence of additives. Ind Eng Chem Res 2011;50(13):8344–53.
[134] Andersson Vibeke, Gudmundsson Jón Steinar. Flow properties of hydrate-in-water slurries. Ann N Y Acad Sci 2000;912:322–9.

[135] Wuchang Wang, Shuanshi Fan, Deqing Liang, et al. Experimental study on flow characters of CH_3CCl_2F hydrate slurry. Int J Refrig 2008;31(3):371–8.

[136] Fukushima S, Shingo Takao, Hdiemasa Ogoshi, et al. Development of high-density cold latent heat with clathrate hydrate. NKK Tech Rep 1999;166: 65–70.

[137] Darbouret Myriam, Cournil Michel, Jean-Michel. Rheological study of TBAB hydrate slurries as secondary two-phase refrigerants. Int J Refrig 2005;28 (5):663–71.

[138] Hashimoto S, Kawamura K, Ito H, et al. Rheological study on tetra-n-butyl ammonium salt semi-clathrate hydrate slurries. In: Proceedings of 7th international conference on gas hydrates. Edinburgh, Scotland; 2011.

[139] Pascal Claina, Anthony Delahaye, Laurence Fournaison, et al. Rheological properties of tetra-n-butylphosphonium bromide hydrate slurry flow. Chem Eng J 2012;193–194:112–22.

[140] Yakushev VS, Istomin VA. Physics and chemistry of ice. Sapporo, Japan: Hokkaido University Press; 1992; 136.

[141] Paul Handa Y, Mishima Osamu, Whalley Edward. Highdensity amorphous ice. III. Thermal properties. J Chem Phys 1986;84(5):2766–70.

[142] Melnikov VP, Nesterov AN, Reshetnikov AM, et al. Stability and growth of gas hydrates below the ice–hydrate–gas equilibrium line on the P–T phase diagram. Chem Eng Sci 2010;65:906–14.

[143] Buchanan P, Soper AK, Thompson HH, et al. Search for memory effects in methane hydrate: structure of water before hydrate formation and after hydrate decomposition. J Chem Phys 2005;125(16):164507–15.

[144] Duchateau C, Glenat P, Pou TE, et al. Hydrate precursor test method for the laboratory evaluation of kinetic hydrate inhibitors. Energy Fuels 2010;24: 616–23.

[145] Wilson PW, Haymet ADJ. Hydrate formation and re-formation in nucleating THF/water mixtures show no evidence to support a memory effect. Chem Eng J 2010;161:146–50.

[146] Qiang Wu, Baoyong Zhang. Memory effect on the pressure-temperature condition and induction time of gas hydrate nucleation. J Nat Gas Chem 2010;19:446–51.

[147] Sefidroodi Hamidreza, Abrahamsen Eirin, Kelland Malcolm A. Investigation into the strength and source of the memory effect for cyclopentane hydrate. Chem Eng Sci 2013;87:133–40.

[148] Sun DL, Wu Q, Zhang BY. Influence of memory effect on induction time of gas hydrate formation. J Harbin Inst Technol 2006;12:2177–9.

[149] Jacobson LC, Hujo W, Molinero V. Amorphous precursors in the nucleation of clathrate hydrates. J Am Chem Soc 2010;132(33):11,806–11.

[150] Tegze G, Gránásy L, Kvamme B. Phase field modeling of CH_4 hydrate conversion into CO_2 hydrate in the presence of liquid CO_2. Phys Chem Chem Phys 2007;9:3104–11.

[151] Qing Yuan, Changyu Sun, Xin Yang, et al. Recovery of methane from hydrate reservoir with gaseous carbon dioxide using a three-dimensional middle-size reactor. Energy 2012;40:47–58.

[152] Yingxia Qi, Masahiro Ota, Hua Zhang. Molecular dynamics simulation of replacement of CH_4 in hydrate with CO_2. Energy Convers Manag 2011;52: 2682–7.

[153] Seungmin Lee, Sungwon Park, Youngjun Lee, et al. Thermodynamic and ^{13}C NMR spectroscopic verification of methane–carbon dioxide replacement in natural gas hydrates. Chem Eng J 2013;225:636–40.

[154] Brown DE, George SM. Surface and bulk diffusion of $H_2^{18}O$ on single-crystal $H_2^{16}O$ multilayers. J Phys Chem 1996;100:15460–9.

[155] Livingston FE, Whipple GC, George SM. Diffusion of HDO into single-crystal $H_2^{16}O$ ice multilayers: comparison with $H_2^{18}O$. J Phys Chem B 1997;101: 6127–31.

[156] Wang XP, Schultz AJ, Halpern Y. Kinetics of methane hydrate formation from polycrystalline deuterated ice. J Phys Chem A 2002;106:7304–9.

[157] Qing Yuan, Changyu Sun, Bei Liu, et al. Methane recovery from natural gas hydrate in porous sediment using pressurized liquid CO_2. Energy Convers Manag 2013;67:257–64.

[158] Fleyfel F, Devlin JP. Carbon dioxide clathrate hydrate epitaxial growth: spectroscopic evidence for formation of the simple type-II CO_2 hydrate. J Phys Chem 1991;95:3811–5.

[159] Englezos Peter. Clathrate hydrate. Ind Eng Chem Res 1993;32:1251–74.

[160] Yoshioki Shuzo. A note on transformation between clathrate hydrate structures I and II. J Mol Graphics Modell 2010;29:290–4.

[161] Yoshioki Shuzo. Identification of a mechanism of transformation of clathrate hydrate structures I to II or H. J Mol Graphics Modell 2012;37:39–48.

[162] Jong-Won Lee, Do-Youn Kim, Huen Lee. Phase behavior and structure transition of the mixed methane and nitrogen hydrates. Korean J Chem Eng 2006;23(2):299–302.

[163] Al-Otaibi Faisal, Clarke Matthew, Maini Brij, et al. Kinetics of structure II gas hydrate formation for propane and ethane using an in-situ particle size analyzer and a Raman spectrometer. Chem Eng Sci 2011;66:2468–74.

[164] Eslamimanesh Ali, Mohammadi Amir H, Richon Dominique. Thermodynamic modeling of phase equilibria of semi-clathrate hydrates of CO_2, CH_4, or N_2+tetra-n-butylammonium bromide aqueous solution. Chem Eng Sci 2012;81:319–28.

[165] Strobel TA, Koh CA, Sloan ED. Hydrogen storage properties of clathrate hydrate materials. Fluid Phase Equilib 2007;261(1/2):382–9.

[166] Changyu Sun, Wenzhi Li, Xin Yang. Progress in research of gas hydrate. Chin J Chem Eng 2011;19(1):151–62.

[167] Ziad Youssef, Anthony Delahaye, Li Huang. State of the art on phase change material slurries. Energy Convers Manag 2013;65:120–32.